



## Article

# Effects of Bone Marrow Sparing and TGF- $\beta$ 3 Treatment in Total Body Irradiation of C57BL/6J Mice

Ingunn Hanson , Jenny T. Vatne and Nina F. J. Edin \*

Department of Physics, University of Oslo, 0371 Oslo, Norway; ingunn.hanson@fys.uio.no (I.H.)

\* Correspondence: n.f.j.edin@fys.uio.no

**Abstract:** Introduction: Mortality from acute radiation syndrome is frequently caused by hematopoietic or gastrointestinal radiotoxicity, the latter of which currently has no effective treatment. Transforming growth factor-beta 3 (TGF- $\beta$ 3) may decrease the severity of radiation-induced gastrointestinal damage in mice. In addition, treatment with TGF- $\beta$ 3 may alleviate radiation-induced fibrosis. Objectives: The current study aimed to investigate the effect of TGF- $\beta$ 3 treatment on acute and late radiotoxicity in whole body irradiated mice. Methods: C57BL/6J mice were total body irradiated with 8.5 Gy X-rays with or without shielding of one hind leg to alleviate hematopoietic radiotoxicity. The effects of intravenous TGF- $\beta$ 3 treatment were investigated. Body weight and pain expression were monitored. Intestine, lung, and liver tissues were preserved and analyzed. Alpha smooth muscle actin ( $\alpha$ -SMA) expression in MRC-5 cells after 3.5 Gy X-irradiation combined with TGF- $\beta$ 3 treatment was analyzed using flow cytometry. Results: All total body irradiated animals died within ten days after irradiation. Ninety-three percent of femur-shielded mice survived until sampling or termination. No effect of TGF- $\beta$ 3 treatment was observed in either group. No increase in collagen content was detected in the lungs or liver from irradiated mice regardless of TGF- $\beta$ 3 treatment. In vitro,  $\alpha$ -SMA expression increased synergistically after irradiation and TGF- $\beta$ 3 treatment. Conclusions: Shielding of the femur during total body irradiation decreased acute gastrointestinal radiation toxicity and increased survival. TGF- $\beta$ 3 treatment did not impact symptoms or survival. TGF- $\beta$ 3 treatment and irradiation increased  $\alpha$ -SMA expression in MRC-5 cells synergistically.

**Keywords:** acute radiation syndrome; radiation-induced fibrosis; radiomitigation; radioprotection; transforming growth factor-beta 3



**Citation:** Hanson, I.; Vatne, J.T.; Edin, N.F.J. Effects of Bone Marrow Sparing and TGF- $\beta$ 3 Treatment in Total Body Irradiation of C57BL/6J Mice. *Appl. Biosci.* **2024**, *3*, 165–185. <https://doi.org/10.3390/applbiosci3020011>

Academic Editor: Demetrios A. Arvanitis

Received: 16 January 2024

Revised: 4 March 2024

Accepted: 29 March 2024

Published: 4 April 2024



**Copyright:** © 2024 by the authors. Licensee MDPI, Basel, Switzerland. This article is an open access article distributed under the terms and conditions of the Creative Commons Attribution (CC BY) license (<https://creativecommons.org/licenses/by/4.0/>).

## 1. Introduction

Incidents involving accidental or intentional exposure to ionizing radiation have the potential to affect large populations in a mass-casualty event. Such incidents may result in acute radiation syndrome (ARS) in individuals who have been exposed to large, acute doses to a significant portion of the body. The clinical course and prognosis of ARS strongly depends on radiation dose and distribution. Clinically, ARS is classified into subsyndromes based on symptoms originating from specific tissues or organs. However, several tissues and organs, and thereby several subsyndromes, may be involved simultaneously [1].

In humans, the hematopoietic subsyndrome (H-ARS) is the major contributor to mortality after total body doses between approximately 2 and 6 Gy [1,2]. Doses between 6 and 10 Gy causes severe gastrointestinal injury (GI-ARS) in addition to H-ARS [1,2]. Mortality from GI-ARS occurs within 3–10 days after exposure, compared to H-ARS which causes mortality within 30–60 days in humans and 10–15 days in mice [2]. In humans, doses above 10 Gy are considered supralethal, manifest a combination of subsyndromes including the neurovascular subsyndrome at doses above 20 Gy, and entail 100% mortality [1,3].

There are currently five available medical countermeasures against ARS approved by the US Food and Drug Administration, all of them targeting H-ARS [4–8]. There are currently no available treatment options specific to GI-ARS or for ARS as a whole [9]. The

demand for such treatments warrants a better understanding of the interplay between H-ARS and GI-ARS.

In addition to potentially lethal acute effects, large doses of ionizing radiation can lead to severe late effects. Radiation-induced fibrosis (RIF) may develop when healthy tissue is replaced by connective tissue following a prolonged inflammatory process and activation of myofibroblasts after radiation damage [10]. RIF is considered an irreversible condition which may affect any organ within the radiation field including skin and lungs, and may considerably affect the quality of life of patients after thoracic radiation therapy [11].

Transforming growth factor-beta 3 (TGF- $\beta$ 3) is a multifunctional, ubiquitously expressed cytokine belonging to the TGF- $\beta$  family of proteins. The three TGF- $\beta$ s (TGF- $\beta$ 1-3) share a high degree of structural similarity [12,13] and signal through the same receptor complexes in similar manners [14,15], but possess distinct functional properties [16–18]. TGF- $\beta$ 3 has been shown to play a role in diverse physiological and pathological processes including embryo development, immunoregulation, and growth regulation and carcinogenesis [17,19–21].

Previous studies have indicated radioprotective effects of TGF- $\beta$ 3 [18]. In vitro, TGF- $\beta$ 3 was shown to decrease the radiosensitivity of rat intestinal epithelioid cells (IEC-6) and increase the radiosensitivity of human colon adenocarcinoma cells (WiDr), measured through cell survival [22]. The modulation of in vitro radiosensitivity was found to depend on the induction of a transient G1/S cell cycle arrest [23–25]. TGF- $\beta$ 3 was also shown to increase the radioresistance of T-47D and T98G cells by removing the default low-dose hyper-radiosensitive response [26,27]. In vivo, treatment with TGF- $\beta$ 3 reduced GI damage and increased survival in BDF1 mice after 12–16 Gy abdominal irradiation [28,29]. In an unpublished pilot study, we found that treatment with TGF- $\beta$ 3 significantly increased survival after a 10.5 Gy total body irradiation (TBI) dose in DBA/2 mice (Supplementary S1: Pilot Study). Furthermore, TGF- $\beta$ 3, in contrast to TGF- $\beta$ 1, is generally considered to be an antifibrotic cytokine, and treatment with TGF- $\beta$ 3 was shown in one study to reduce the severity of radiation-induced pulmonary fibrosis in C57BL/6 mice [30].

The aim of the current study was to investigate whether treatment with TGF- $\beta$ 3 could alleviate symptoms of ARS and increase survival when administered before or after an 8.5 Gy total body dose. Bone marrow (BM) was spared through limb shielding to alleviate H-ARS and distinguish it from GI-ARS. Surprisingly, no effect was observed from TGF- $\beta$ 3 treatment in any of the groups. BM sparing was found to decrease symptoms of GI-ARS and increase survival. Furthermore, the effects of TGF- $\beta$ 3 treatment on fibrogenesis were studied in surviving animals and in vitro. Whereas no increase in collagen deposition was discovered in the lungs or liver of surviving BM-spared mice regardless of TGF- $\beta$ 3 treatment, expression of the early fibrosis marker  $\alpha$ -SMA in MRC-5 cells increased when TGF- $\beta$ 3 treatment was combined with irradiation.

## 2. Materials and Methods

### 2.1. Cell Culture and Treatment

Human lung fibroblast cell line MRC-5 cells [31] (ECACC MRC-5 pd30, purchased from Sigma, Saint-Louis, MO, USA, December 2011) were grown as monolayer cultures in 5 mL Eagle's minimum essential medium (Euroclone, Milan, Italy) supplemented with 10% fetal calf serum (Euroclone, Milan, Italy), 2 mM l-glutamine, and 1% penicillin/streptomycin (both from Gibco, Baltimore, MD, USA) per 25 cm<sup>2</sup> flask (Nunc A/S, Roskilde, Denmark) in air containing 5% CO<sub>2</sub> at 37 °C. Cells were recultivated twice per week with an additional medium change once per week. TGF- $\beta$ 3 treated cells were incubated with recombinant TGF- $\beta$ 3 (R&D Systems, Minneapolis, MN, USA) in cell medium at concentrations of 0.01 ng/mL, 0.5 ng/mL, or 50 ng/mL for 72 h. Cells were irradiated with 3.5 Gy 220 kV X-rays filtered by 1.52 mm Al and 0.7 mm Cu filters delivered at a dose rate of 35.4 Gy/h in an irradiation chamber heated to 37 °C. Control cells were sham-irradiated according to the same procedure.

## 2.2. $\alpha$ -SMA Detecting Assay

A detailed protocol can be found in Supplementary S2:  $\alpha$ -SMA detection protocol. Briefly, fresh MRC-5 cells were seeded 96 h before analysis, treated with TGF- $\beta$ 3 72 h before analysis, and irradiated 48 h before analysis. TGF- $\beta$ 3 treatment was tested at different concentrations based on previous work from our laboratory to establish a dose–response relationship [26]. Cells were then trypsinated and washed with PBS (both from Lonza, Walkersville, MD, USA), and stained with anti- $\alpha$ -SMA (ab 150301, Abcam, Cambridge, UK) diluted 1:600 in PBS with 1% BSA (Merck, Rahway, NJ, USA). Before staining, samples were split in two, and secondary antibody controls were incubated in PBS with 1% BSA. Cells were then washed and stained with IgG goat anti-rabbit Alexa Fluor™ 647 secondary antibody (A-21244, Invitrogen, Waltham, MA, USA) diluted 1:400 in PBS with 1% BSA. Finally, live/dead staining was performed by staining with 3.2  $\mu$ g/mL propidium iodide (Sigma Aldrich, Saint-Louis, MO, USA). All centrifuge steps were performed at 200 $\times$  *g* for 5 min. Samples were analyzed using an Accuri C6 flow cytometer (BD Biosciences, Franklin Lakes, NJ, USA).

## 2.3. Animals

All procedures involving animals were approved by the Norwegian Food Safety Authority (FOTS ID 25032) according to the EU directive 2010/63. All researchers handling animals held FELASA (Federation of Laboratory Animal Science Associations) C certification. Thirty 10-week-old female C57BL/6J mice weighing 16–22 g were obtained from Janvier (Le Genest-Saint-Isle, France). No exclusion criteria were determined a priori, and no animals were excluded from the experiment. The animals were housed in cages of six and kept in a 12 h light/12 h dark cycle under pathogen-free conditions with standard commercial fodder and water given ad libitum. Cages contained nesting material and refuge. Animals were acclimatized for one week before the initiation of the experiment. One mouse from each cage was randomly assigned to each of the six experimental groups (n = 5 mice per group). A power analysis based on results from an unpublished pilot study was used to determine the appropriate group size.

## 2.4. Treatment

The groups and treatment protocol are represented in Figure 1. Groups A, B, and C received one total body 225 kV X-ray dose of 8.5 Gy at a dose rate of 59 Gy/h using a Faxitron Multirad225 irradiation system (Faxitron Bioptics, Tucson, AZ, USA). For the animals in groups D, E, and F, the same dose was given with a lead shield placed over the left hind leg, to shield the femur from radiation. The dose was chosen based on previous reports of the dose response of C57BL/6 mice to approximate an LD<sub>90/30</sub> value [32,33]. Groups B and E received one i.v. tail vein injection of 0.1 mL saline containing 2.5  $\mu$ g/mL recombinant TGF- $\beta$ 3 (R&D systems, Minneapolis, MN, USA) 24 h before irradiation, while groups C and F received the same injection 24 h after irradiation. Groups A and D received one 0.1 mL i.v. tail vein injection of vehicle 24 h before irradiation. The TGF- $\beta$ 3 dose was chosen based on the results from the pilot study (Supplementary S1: Pilot study). All animals were gas anesthetized (Sevoflurane 4% in O<sub>2</sub>) during irradiation and i.v. injection. Mice were treated in the order of the groups, researchers were not blinded, and potential confounders were not controlled.

Group	Day -1	Day 0	Day 1	Day 10	Day 73	Day 110
A		Total body irradiation		0 % survival		
B	i.v. TGF- $\beta$ 3	Total body irradiation		0 % survival		
C		Total body irradiation	i.v. TGF- $\beta$ 3	0 % survival		
D		Irradiation w/ shielded femur			Sampling	100 % survival
E	i.v. TGF- $\beta$ 3	Irradiation w/ shielded femur		80 % survival	Sampling	80 % survival
F		Irradiation w/ shielded femur	i.v. TGF- $\beta$ 3		Sampling	100 % survival

**Figure 1.** Overview of the groups A–F and treatment including intravenous (i.v.) TGF- $\beta$ 3 injections and total body irradiation with or without shielding of the left femur.

### 2.5. Follow-Up

The primary outcome measure for the study was survival and humane endpoints were established to minimize animal suffering. Secondary outcome measures included pain expression, body temperature, body weight, clinical symptoms and necropsy remarks, small intestine pathology, and lung and liver collagen content.

Welfare checks were performed twice per day for the first 30 days after irradiation, and daily for the remainder of the experiment period of 110 days. Pain was scored according to a scale developed by Nunamaker et al. [34] by observing mice in the cage. Body temperature was measured using an infrared non-contact thermometer (Brannan, Cleator Moor, UK) pointing to the abdomen and involved temporary fixation of the animals. Mice were weighed at least twice per week, and more frequently upon indication. Humane endpoints were defined as meeting one or more of the following criteria: (1) A pain score of 7, (2) a 30% reduction in body temperature relative to baseline, or (3) a 20% and increasing decline in body weight relative to baseline. Due to the severe nature of ARS symptoms and the low likelihood of recovery, euthanasia was considered more humane than analgesic treatment. Two mice were found dead in the cage despite not having met any of the humane endpoints at the previous welfare check. The remainder were euthanized by cervical dislocation within 30 min after meeting one of the humane endpoints, for sampling on day 73, or after termination of the experiment on day 110. A diagnostic necropsy was performed immediately after euthanasia.

### 2.6. Histological Evaluations

Immediately after euthanasia, the lungs, liver, and small intestine were collected and preserved in formalin (Sigma Aldrich, Saint-Louis, MO, USA). Paraffin embedding, sectioning, and H&E staining were performed at the Department of Pathology, Oslo University Hospital. Staining with Masson's Trichrome Stain Kit (Abcam, Cambridge, UK) was performed according to the manufacturer's instructions at the Department of Oral Biology, University of Oslo. H&E sections of the small intestine were examined using a Nikon E90i microscope. Masson's Trichrome-stained sections of lungs and liver were scanned using a SLIDEVIEW™ VS200 slide scanner (Olympus, Tokyo, Japan). The images were processed in Qupath [35], and collagen was quantified using the Color Threshold function in ImageJ [36]. A detailed image analysis protocol was previously published in [37]. Researchers were blinded during histological data analysis.

For the analysis of small intestine morphology and collagen content in the lungs and liver, two non-irradiated, age- and sex-matched mice from another experiment were included as negative controls. These animals were sham-irradiated under gas anesthesia 105 days before euthanasia by intraperitoneal anesthetic injection (Pentobarbital, Exagon® Vet, Richter Pharma AG, Wels, Austria).

## 2.7. Statistical Analyses

Statistical analyses were performed using Microsoft Excel and the following online statistics software: Kendall's  $\tau$  [38]. The survival data in Figure 4 were analyzed using a log-rank test with a significance level of  $p = 0.05$ . The correlations in Figure 6 were analyzed using Kendall's  $\tau$ . The correlation data in Figure 9 were analyzed using the point-biserial correlation coefficient. The  $\alpha$ -SMA expression data in Figure 13 were analyzed using one-way ANOVA with a post hoc Tukey test. A significance level of  $p = 0.05$  was applied in all cases except for Figure 4B, where the Bonferroni correction for multiple comparisons was used by adjusting the significance level to  $p = 0.0033$  for 15 comparisons between treatment groups.

## 3. Results

### 3.1. Acute Effects and Survival after 8.5 Gy Irradiation

In this study, the effect of TGF- $\beta$ 3 treatment on survival after large, acute doses of X-radiation was studied in C57BL/6J mice. To evaluate the effect of TGF- $\beta$ 3 treatment in the hematopoietic versus the gastrointestinal subsyndrome of ARS, three groups were irradiated with a shielded femur to spare BM, while three groups were TBI with the same dose of 8.5 Gy.

The majority of animals in the BM-spared groups D, E, and F displayed a moderate weight loss from day 5 after irradiation, but recovered within day 10 (Figure 2A). No differences in weight loss were observed between the three groups. BM-spared animals scored moderately high in pain with a peak around day 10, before recovering within day 15 (Figure 2B), regardless of TGF- $\beta$ 3 treatment. Instances of moderate pain in individual animals were noted later in the experiment but with no time-dependent pattern within or between groups.

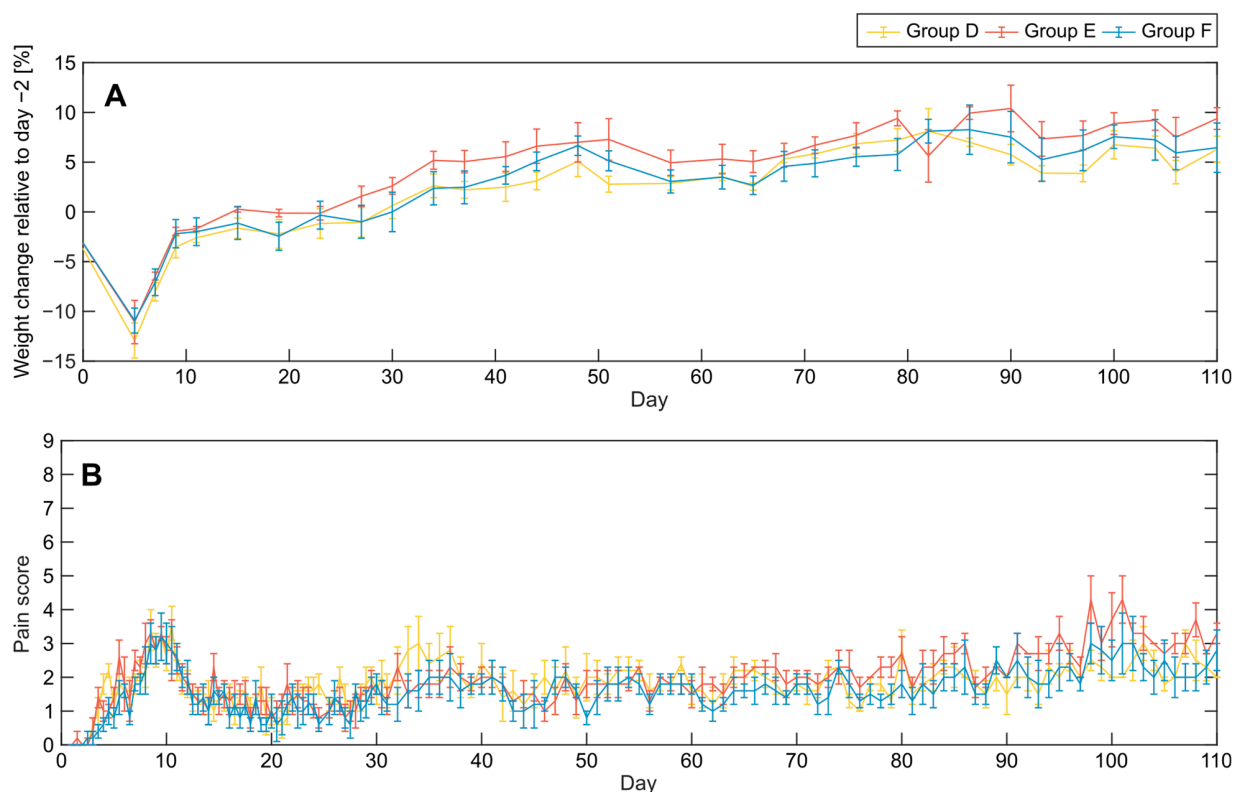


**Figure 2.** Weight change and pain score: BM-spared mice. (A) Mean change in body weight relative to day -2 before irradiation for animals in groups D (yellow), E (red), and F (blue) ( $n = 5$  for each group). (B) Mean pain score as defined in [34] for the same groups as A. Error bars represent the standard error of the mean (SEM).

The animals in the TBI groups A, B, and C rapidly lost weight from around day 5 after irradiation (Figure 3A), and simultaneously exhibited indications of increasing pain (Figure 3B). No differences between groups A, B, and C were observed for weight loss or pain score.

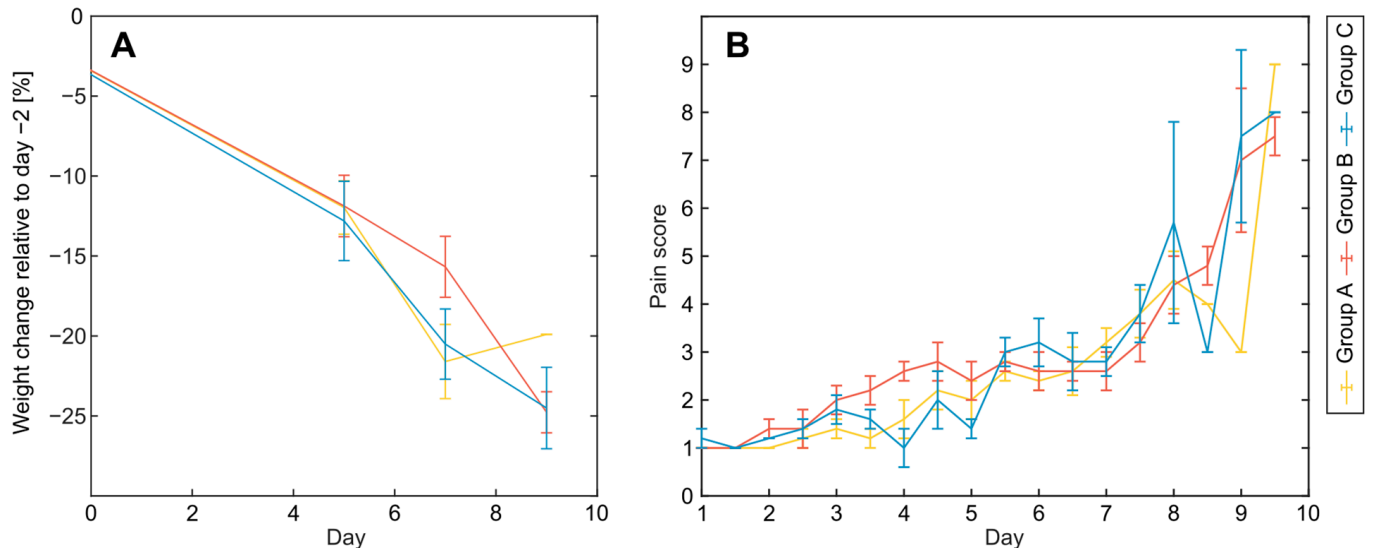


**Figure 3.** Weight change and pain score: TBI mice. (A) Mean change in body weight relative to day  $-2$  before irradiation for animals in groups A (yellow), B (red), and C (blue) ( $n = 5$  for each group). (B) Mean pain score as defined in [34] for the same groups as A. Error bars represent SEM. All TBI animals had died by day 10.

Survival differed significantly ( $p = 0.000038$ , log-rank test) between BM-spared and TBI animals (Figure 4A). One mouse from group A and one from group B died spontaneously on day 8 and day 9, respectively, without reaching any of the humane endpoints at the previous welfare check. The remaining TBI mice were all euthanized by day 10 after reaching one or more humane endpoints. One mouse in group E experienced severe and progressing weight loss and was euthanized on day 6. The remaining BM-spared mice survived until being sacrificed for sampling on day 73 (one mouse each from groups D, E, and F) or termination of the experiment on day 110 (Figure 4B). TGF- $\beta 3$  treatment did not impact survival in the BM-spared or the TBI groups.

Body temperature measurements fluctuated with no clear time-dependent patterns throughout the experiment for any of the treatment groups. No differences in body temperature measurements were detected between any of the treatment groups (Figure 5). Weak negative correlations were found for both TBI and BM-spared animals between temperature change and pain score (TBI animals: Kendall's  $\tau$  value  $-0.18$ ,  $p = 0.00066$ ; BM-spared animals: Kendall's  $\tau$  value  $-0.20$ ,  $p < 0.0001$ ), and between temperature change and change in body weight (TBI animals: Kendall's  $\tau$  value  $-0.22$ ,  $p = 0.0087$ ; BM-spared animals: Kendall's  $\tau$  value  $-0.1$ ,  $p = 0.0036$ ) (Figure 6). No correlation was found between change in body temperature and survival.

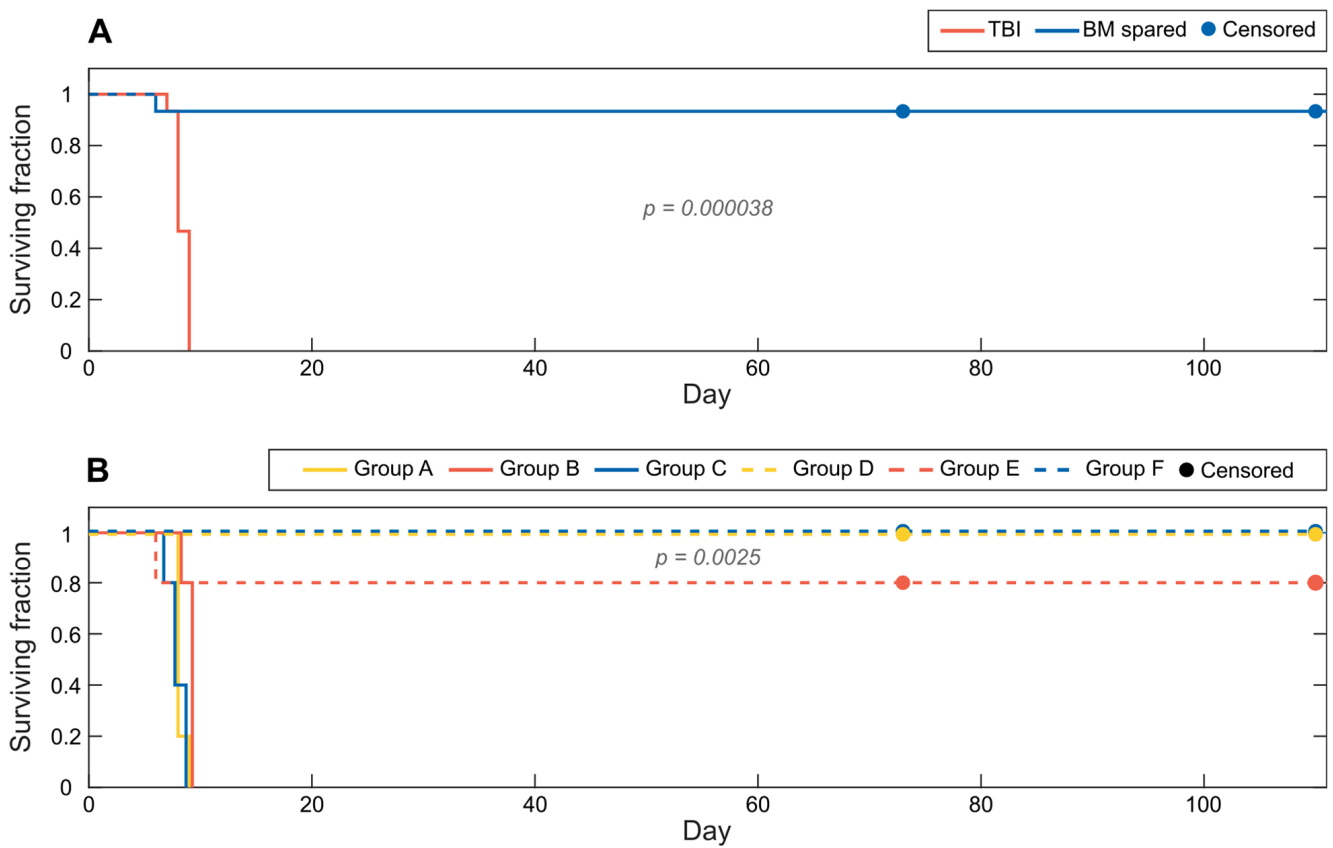


**Figure 4.** Survival after 8.5 Gy irradiation. **(A)** Pooled survival for TBI animals (groups A, B, and C: Red) and BM-spared animals (groups D, E, and F: Blue), regardless of TGF- $\beta$ 3 treatment ( $n = 15$  for both groups). Censored events: euthanasia at sampling point (day 73) and termination of the experiment (day 110). The difference in survival was significant ( $p = 0.000038$ , log-rank test). **(B)** Survival for animals in groups A (solid yellow), B (solid red), C (solid blue), D (dashed yellow), E (dashed red), and F (dashed blue).  $n = 5$  for each group. Censored events: euthanasia at the sampling point and termination of the experiment. The family-wise comparison was significant ( $p = 0.0025$ , log-rank test). However, neither pair-wise comparison reached significance after applying the Bonferroni correction for  $n = 15$  comparisons.

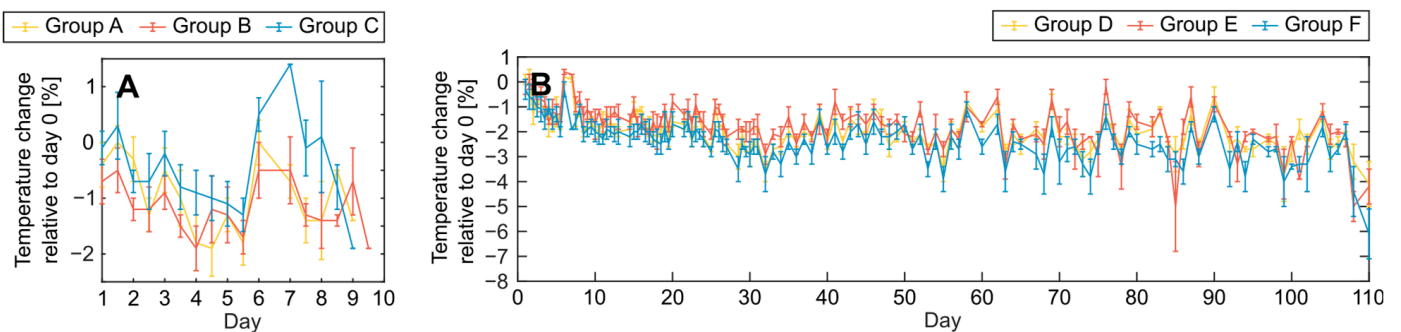


**Figure 5.** Body temperature. **(A)** Mean change in body temperature relative to day 0 for TBI animals in group A (yellow), B (red), and C (blue) ( $n = 5$  for each group). **(B)** Mean change in body temperature relative to day 0 for BM-spared animals in group D (yellow), E (red), and F (blue) ( $n = 5$  for each group). Error bars represent SEM.

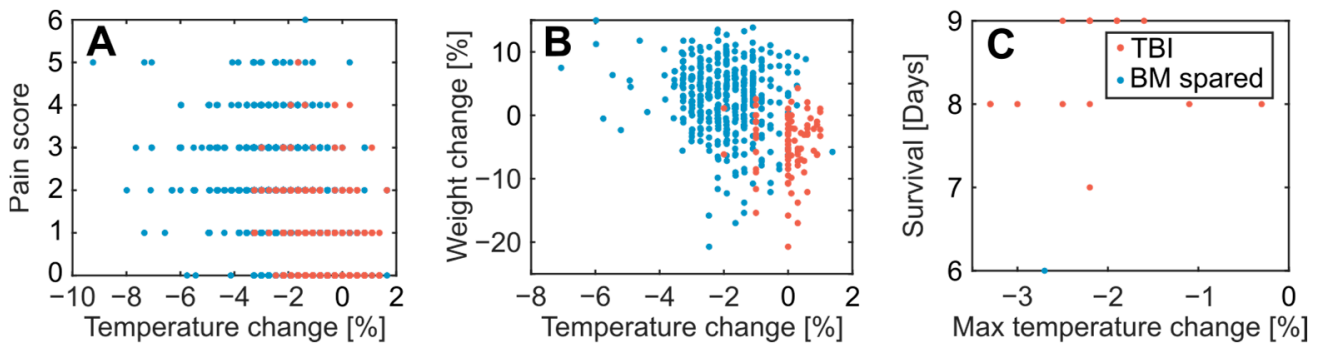


**Figure 6.** Body temperature: Correlations with other parameters. **(A)** Pain score vs. change in body temperature relative to day 0, for TBI (red) and BM-spared (blue) animals ( $n = 15$  for each). Each point represents one welfare check for one animal. Weak negative correlations were found for both groups (TBI: Kendall’s  $\tau -0.18$ ,  $p = 0.00066$ ; BM-spared: Kendall tau  $-0.20$ ,  $p < 0.0001$ ). Note that pain scores  $\geq 7$  are not included, as animals that reached this humane endpoint were euthanized immediately without body temperature measurement. **(B)** Change in body weight relative to day -2 vs. change in body temperature relative to day 0, for TBI (red) and BM-spared (blue) animals ( $n = 15$  for each). Weak negative correlations were found for both groups (TBI: Kendall’s  $\tau -0.22$ ,  $p = 0.0087$ ; BM-spared: Kendall’s  $\tau -0.1$ ,  $p = 0.0036$ ). Only temperature measuring points corresponding to a body weight measurement are included. **(C)**. Survival time vs. maximum registered change in body temperature relative to day 0 for TBI (red) ( $n = 10$ ) and BM-spared (blue) ( $n = 1$ ) animals. Only animals that died spontaneously or reached humane endpoints are included in the analysis. No significant correlation was found. One point represents one (small marker), two (medium marker), or three (large marker) animals.

3.2. Clinical Symptoms and Necropsy Assessments

A timeline of clinical symptoms observed during daily welfare checks is illustrated in Figure 7. During the first 15 days after irradiation, animals from all treatment groups displayed depilation, mainly on the head, back of the neck, and back. In surviving animals, hair growth recovered after the initial depilation. All surviving animals from groups D, E, and F displayed varying degrees of fur depigmentation in the area covered by the radiation field starting from day 19 after irradiation. Representative images of the distinctive depigmentation pattern are displayed in Figure 8.

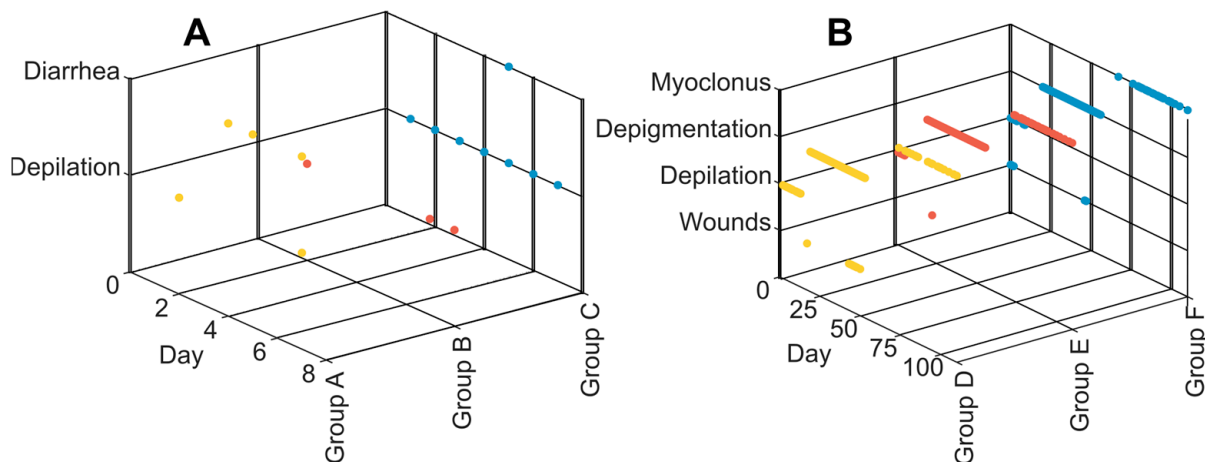


**Figure 7.** Clinical symptoms. **(A)** Clinical symptoms observed in TBI animals (group A (yellow), B (red), and C (blue)) ( $n = 5$  for each group). **(B)** Clinical symptoms observed in BM-spared animals (group D (yellow), E (red), and F (blue)) ( $n = 5$  for each group). Each point symbolizes observance of the symptom in one or more animals from the respective group on the respective day.

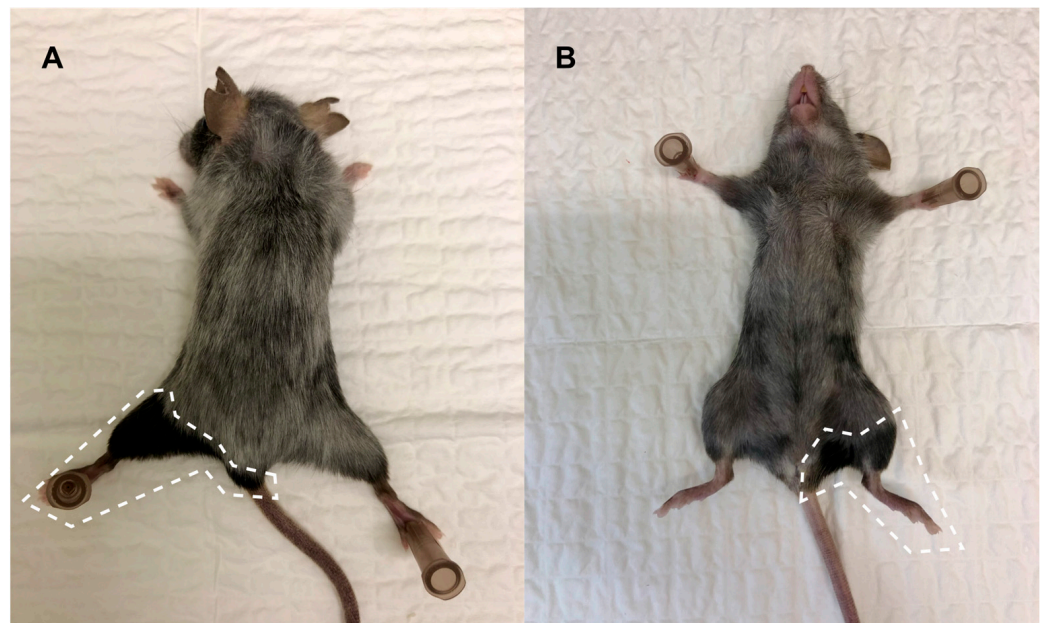


**Figure 8.** Depigmentation in BM-spared animals. (A) Representative posterior image of depigmentation in surviving BM-spared mice. (B) Representative anterior image of depigmentation in surviving BM-spared mice. The dashed white lines indicate the area on the left hind leg that was shielded during irradiation and where depigmentation did not occur.

Observations of diarrhea were made between day 4 and day 7, for three mice from group A and one from group C. However, the animals were not continuously monitored for diarrhea, and it is therefore likely that this clinical symptom went unnoticed in several animals.

Several animals in groups D, E, and F displayed cutaneous wounds between day 17 and day 50 after irradiation. All wounds healed within a few days without intervention and did not appear to increase pain in the animals.

Myoclonus was observed in a majority of the animals in groups D, E, and F in the later stages of the follow-up period, with the first observation on day 67 after irradiation. Occurrence of myoclonus correlated positively with pain score (point-biserial correlation coefficient +0.45,  $p < 0.0001$ ), and weakly with weight gain (point-biserial correlation coefficient +0.16,  $p = 0.00026$ ), Figure 9.

Diagnostic necropsies were performed immediately after euthanasia. One mouse from group A and one from group B were discovered dead in the cage, and a necropsy could not be performed for these animals. For animals dying in the first 10 days after irradiation (all animals in groups A, B, and C, and one from group E), observations indicated severe GI radiation damage. These observations included dehydration and blood in the abdominal cavity, intestines, or stomach (Figure 10I). Other observations in these animals included ulceration in previously mentioned depilated areas or the oral cavity, fluid in the thoracic cavity, discoloration of the lungs, paleness of the liver, and blood in the urinary bladder.

One animal each from groups D, E, and F were sacrificed on day 73 after irradiation, while the remaining were sacrificed on day 110. Necropsies of these animals led to observations of enlarged lymph nodes and discoloration of the lungs in several animals from each group, with no apparent difference between groups (Figure 10II). Animals sacrificed on day 73 displayed a higher incidence of enlarged lymph nodes (67% compared to 27%) and discoloration of lungs (67% compared to 55%).

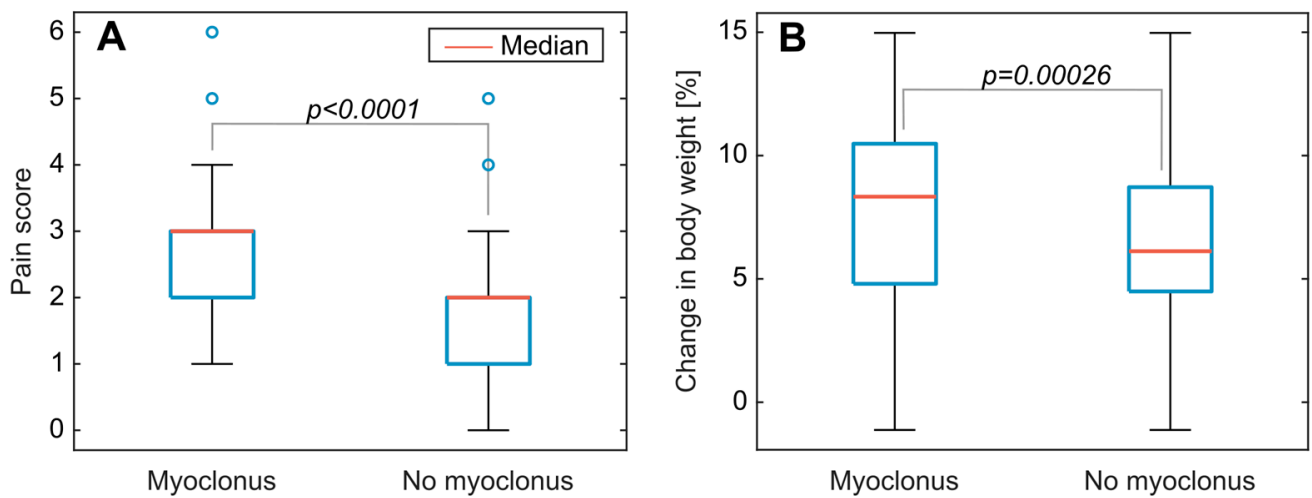


**Figure 9.** Myoclonus in BM-spared mice. **(A)** Pain score on days where myoclonus was registered versus days where no myoclonus was registered, for all surviving BM-spared mice (group D, E, and F) from day 67 after irradiation (n = 14). The presence of myoclonus was positively correlated with pain score (point–biserial correlation coefficient 0.45,  $p < 0.0001$ ). **(B)** Change in body weight relative to day -2 on days where myoclonus was registered versus days where no myoclonus was registered, for all surviving BM-spared mice (group D, E, and F) from day 67 after irradiation (n = 14). For days where body weight was not registered, the previous measuring point was used. Presence of myoclonus was weakly correlated with weight gain (point–biserial correlation coefficient 0.16,  $p = 0.00026$ ). Group medians in red.

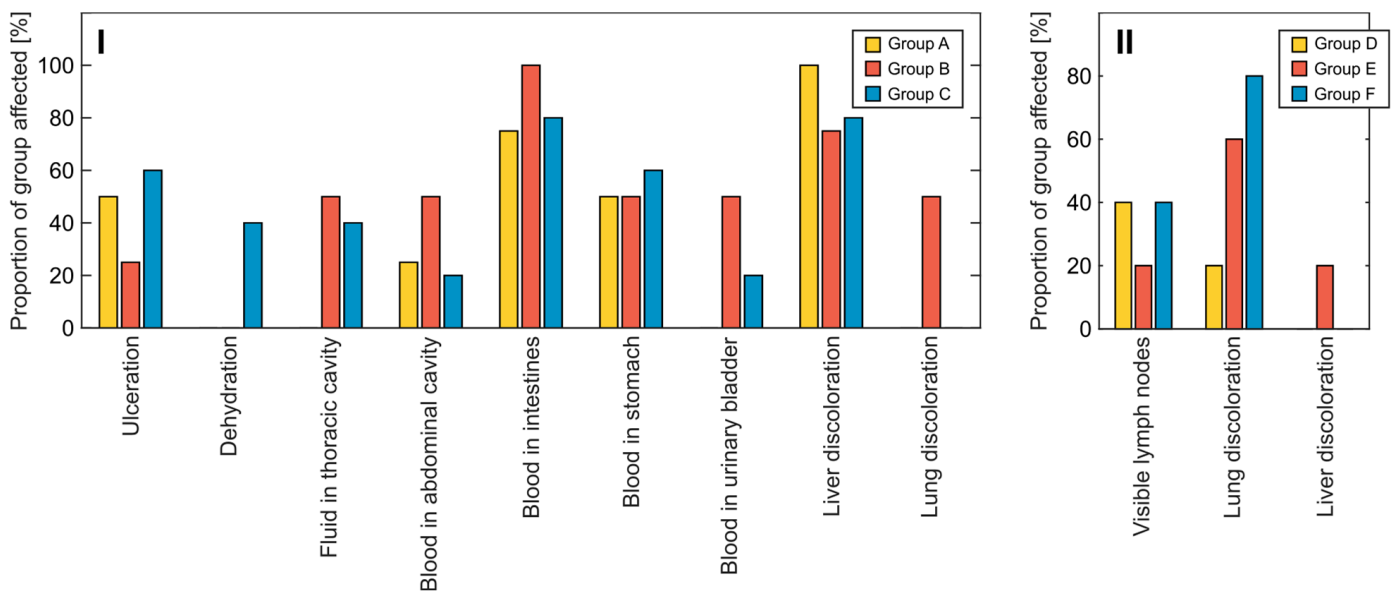


**Figure 10.** Necropsy remarks. **(I)** Overview of necropsy observations in TBI animals in group A (yellow) (n = 4), B (red) (n = 4), and C (blue) (n = 5). One mouse in group A and one in group B died spontaneously and did not undergo necropsy. All TBI mice died by day 10. **(II)** Overview of necropsy observations in BM-spared animals in group D (yellow), E (red), and F (blue) (n = 5 for each). One mouse in group E was euthanized on day 6 due to severe weight loss. The remaining BM-spared animals survived until sampling on day 73 (one mouse from each group) or termination of the experiment on day 110.

### 3.3. Small Intestine Histology

Small intestine from TBI and BM-spared animals were preserved, paraffin-embedded, sectioned, and stained with H&E. These sections were compared with corresponding sections from control animals that were anesthetized and sham-irradiated 105 days before euthanasia [37,39,40]. Tissue was collected after euthanasia within day 10 after irradiation for all TBI animals, and at day 73 or day 110 after irradiation for BM-spared animals.

Representative images of H&E-stained small intestine tissue sections are displayed in Figure 11. For TBI animals, small intestine tissue sections showed a high level of inflammation and an increased number of red blood cells in addition to shortening of the villi and decreased villus density, compared to controls. No evidence of necrotic tissue was found and a normal number of crypts were present in the small intestine of animals euthanized on days 7–9 after irradiation. Crypts were generally less basophilic than in BM-spared and non-irradiated small intestines. Sections from BM-spared animals showed short villi and low villus density compared to controls. No evidence of inflammation was seen in BM-spared small intestine sections at day 73 or 110 after irradiation. In the non-irradiated control animals, villi were of normal length and density.

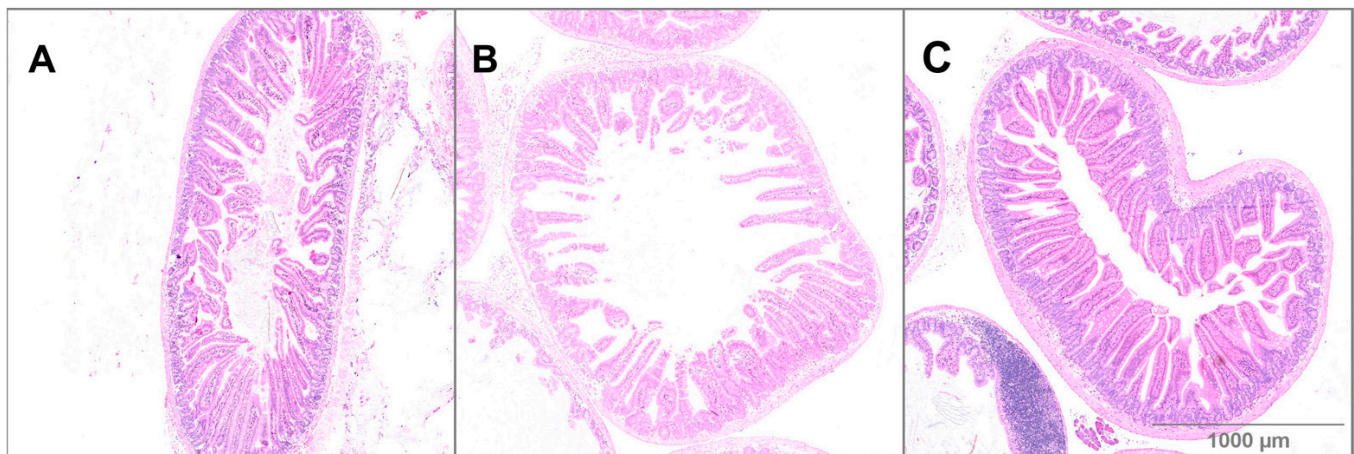


**Figure 11.** Small intestine tissue sections. (A) Representative image of H&E-stained small intestine from a non-irradiated control animal. (B) Representative image of H&E-stained small intestine from TBI animal, sacrificed on day 8 after irradiation. (C) Representative image of H&E-stained small intestine from BM-spared animal, sacrificed on day 110 after irradiation.

### 3.4. In Vitro $\alpha$ -SMA Expression after Treatment with TGF- $\beta$ 3 and Radiation

To analyze the effect of TGF- $\beta$ 3 treatment in combination with irradiation in vitro, the expression of the early fibrosis marker  $\alpha$ -SMA was analyzed in the lung fibroblast cell line MRC-5. TGF- $\beta$ 3 treatment alone did not significantly affect  $\alpha$ -SMA expression at any of the tested concentrations (Figure 12). X-irradiation (3.5 Gy) increased the expression of  $\alpha$ -SMA in MRC-5 cells after 72 h. The increase was present in all experiments and reached significance in one set of experiments, ( $p = 0.001$ , one-way ANOVA with post hoc Tukey test) (Figure 12C). When combined with 3.5 Gy irradiation, TGF- $\beta$ 3 treatment increased the expression of  $\alpha$ -SMA in an apparently dose-dependent manner.

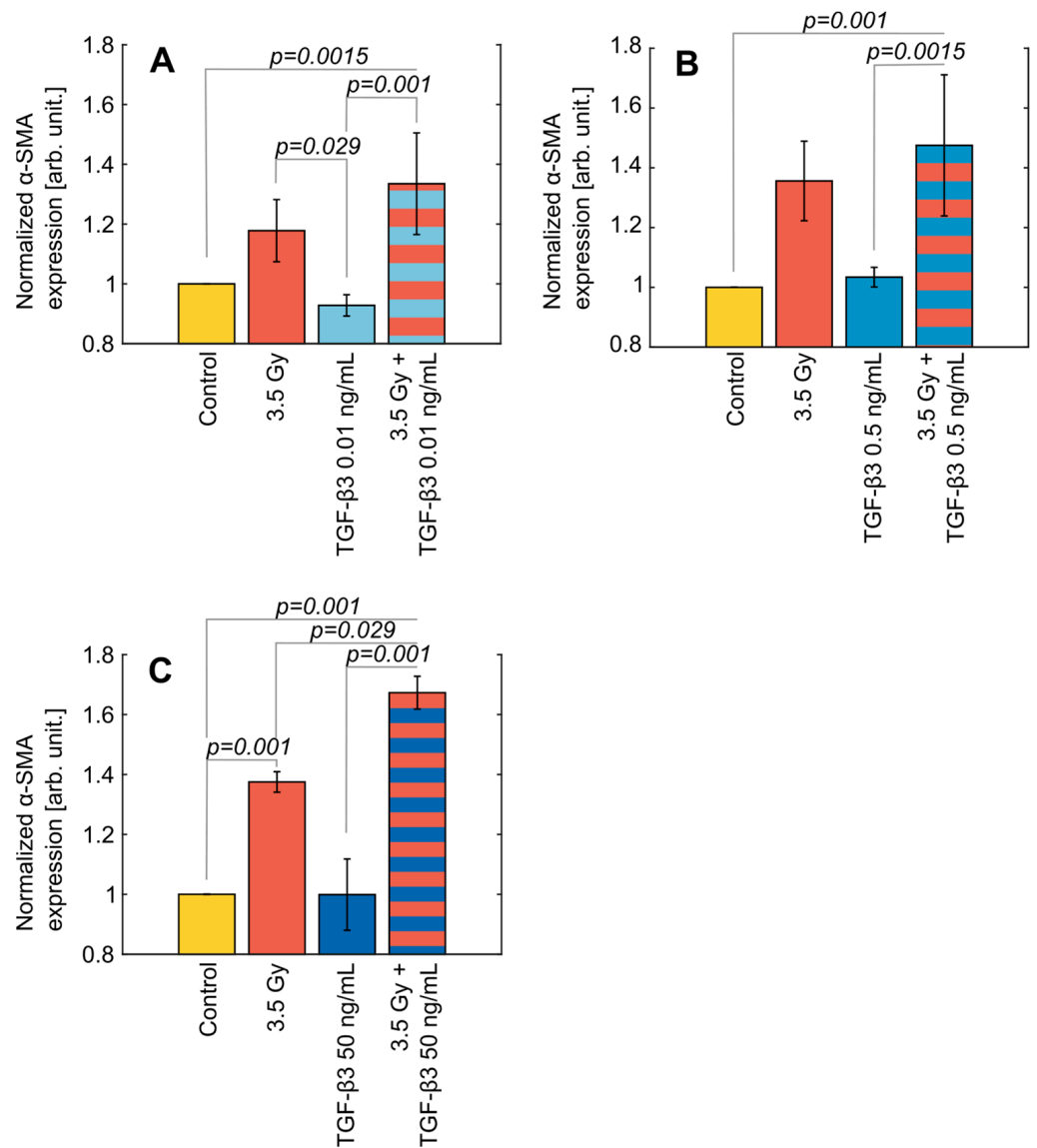


**Figure 12.** In vitro α smooth muscle actin (α-SMA) expression. (A) Normalized error-weighted means of α-SMA expression in MRC-5 cells for untreated and non-irradiated controls (yellow), irradiated cells (red), cells treated with 0.001 ng/mL TGF-β3 (light blue), and irradiated cells treated with 0.001 ng/mL TGF-β3 (striped red and light blue); n = 3 experiments, each with two biological replicates. (B) Normalized error-weighted means of α-SMA expression in cultured MRC-5 cells for non-irradiated controls (yellow), irradiated cells (red), cells treated with 0.05 ng/mL TGF-β3 (medium blue), and irradiated cells treated with 0.05 ng/mL TGF-β3 (striped red and medium blue); n = 3 experiments, each with two biological replicates. (C) Normalized error-weighted means of α-SMA expression in cultured MRC-5 cells for non-irradiated controls (yellow), irradiated cells (red), cells treated with 50 ng/mL TGF-β3 (dark blue), and irradiated cells treated with 50 ng/mL TGF-β3 (striped red and dark blue); n = 5 experiments, each with two biological replicates. TGF-β3 was added to the cell medium 24 h before irradiation. Cells were irradiated 24 h before flow cytometry. All samples were normalized to controls. Error bars represent SEM. Statistical analysis: one-way ANOVA with post hoc Tukey test.

### 3.5. Collagen Content in Lung and Liver Sections from BM-Spared Mice

Tissue sections from the lungs and liver of BM-spared animals sacrificed on days 73 and 110 were stained with Masson’s Trichrome and images were analyzed to measure collagen content. These sections were compared to sections from sham-irradiated control

mice from an earlier study [37,39,40]. The results are displayed in Figure 13. No increase in collagen content was detected for sections of the lungs or liver after 8.5 Gy TBI with shielding of the left hind leg, compared to non-irradiated mice. No effect was seen from TGF- $\beta$ 3 treatment in the irradiated lungs ( $p = 0.97$  for liver sections and  $p = 0.81$  for lung sections, one-way ANOVA).

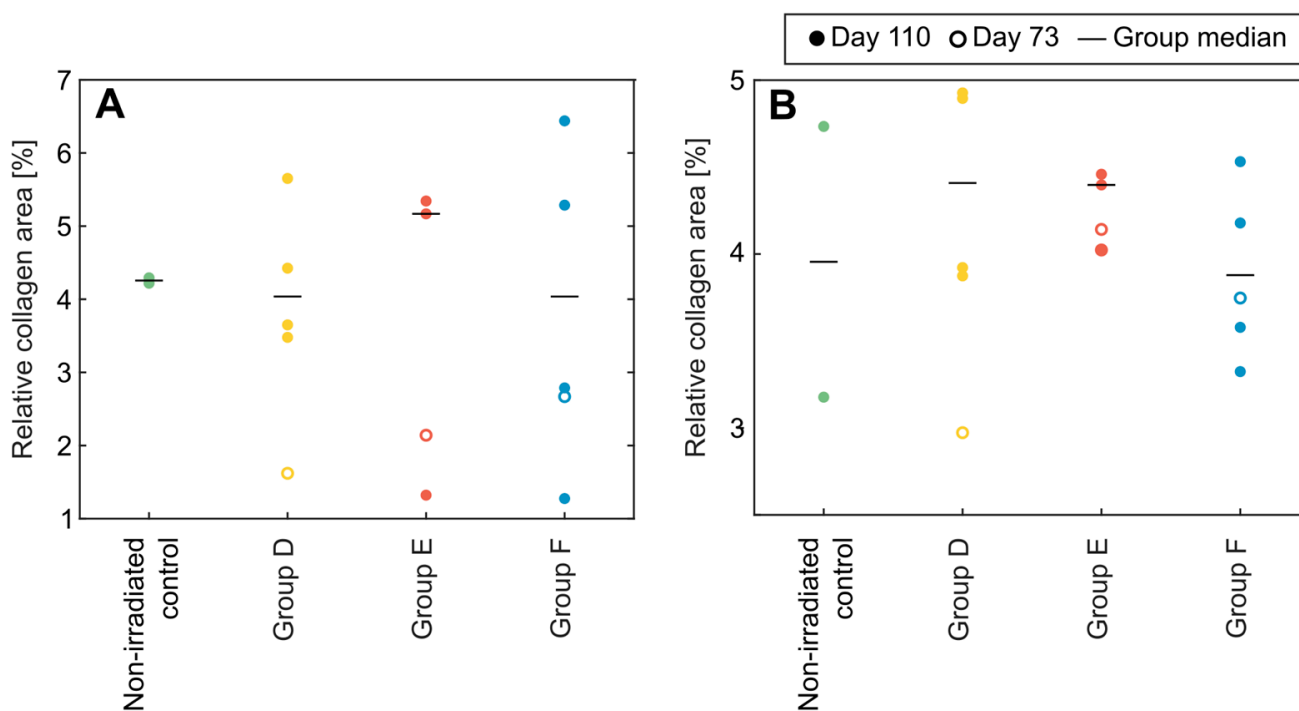


**Figure 13.** Collagen content in tissue from BM-spared animals. (A) Percentage of area stained as collagen relative to total area in liver tissue sections from non-irradiated controls (green) ( $n = 2$ ) and BM-spared animals in group D (yellow) ( $n = 5$ ), group E (red) ( $n = 4$ ), and group F (blue) ( $n = 5$ ). (B) Percentage of area stained as collagen relative to total area in lung tissue sections from non-irradiated controls (green) ( $n = 2$ ) and BM-spared animals in group D (yellow) ( $n = 5$ ), group E (red) ( $n = 4$ ), and group F (blue) ( $n = 5$ ). Each point represents one animal. Circles = sacrificed on day 73, solid = sacrificed on day 110. Black lines represent group medians.

#### 4. Discussion

##### 4.1. Acute Effects of Total Body and Bone Marrow-Spared Irradiation

In the current study, C57BL/6J mice subjected to a TBI dose of 8.5 Gy all died or reached humane endpoints within nine days. This, together with the display of severe weight loss, the appearance of diarrhea, and the gross GI damage revealed during necropsies, suggests GI-ARS to be the main cause of mortality. Symptoms of GI-ARS are caused by damage to the epithelium in the GI tract and GI-ARS-caused mortality generally occurs 3–10 days after exposure due to the rapid turnover of GI epithelium [1,2,9].

In the current study, no radioprotective or sensitizing effects could be observed from treatment with TGF- $\beta$ 3 24 h before or after TBI in C57BL/6J mice. This is in contrast to our previously unpublished pilot study (Supplementary S1: Pilot Study), in which a 12.5  $\mu$ g/kg intraperitoneal TGF- $\beta$ 3 injection 24 h after irradiation significantly improved survival after an LD<sub>50</sub> TBI dose in DBA/2 mice. In the pilot study, the median survival of control TBI animals was 76.5 days, with only one death in the first 10 days after irradiation. This indicates a lesser degree of GI-ARS involvement compared to the current study. This difference may in part be explained by a difference in animal model-related radiosensitivity. Due to this difference, the TBI dose was lowered from 10.5 Gy in the pilot study to 8.5 Gy in the current study to achieve similar effects. However, the dose–response relationship for TBI around the LD<sub>50</sub> is very steep for C57BL/6J mice and 8.5 Gy may have caused effects

that were too severe for rescue by TGF- $\beta$ 3 treatment [41]. More importantly, however, the animals in the pilot study were bred and housed in a non-barrier unit which has since been decommissioned. Therefore, the animals in the current experiment were kept in pathogen-free conditions. Considerable gut microbiome variations must therefore be assumed between the animals in the two experiments. It has been well documented that a complete and functional gut microbiome may lower gastrointestinal radiosensitivity, and conversely that ionizing radiation adversely affects the gut microbiome [42–44].

In addition to the above-mentioned pilot study, other studies have demonstrated a protective effect of TGF- $\beta$ 3 treatment on acute radiation-induced GI damage in non-barrier housed mice after abdominal or total body irradiation [28,29]. In one of these studies, TGF- $\beta$ 3 had a radioprotective effect when administered before irradiation, but had a radiosensitizing effect when delivered after irradiation [28]. The lack of radioprotection afforded by TGF- $\beta$ 3 may be explained by several factors. First, the TGF- $\beta$ 3 dose in the current study was lower at ~12.5  $\mu$ g/kg compared to a repeated treatment regime with between four and six injections of 20–100  $\mu$ g/kg in the above-mentioned studies, and may have been insufficient to prevent acute GI damage. Alternatively, the radiation dose used in the current experiment may have been too high to afford prevention of or rescue from GI-ARS. Nevertheless, the gut microbiome status of the animals seems likely to have influenced the radioprotective effect of TGF- $\beta$ 3 in the GI system, an observation that warrants further investigation. Moreover, animal models with complete and functional gut microbiomes may be considered more relevant for human physiology. In humans, topical treatment with recombinant TGF- $\beta$ 3 underwent clinical trials to assess its effect on chemotherapy-induced oral mucositis [45,46]. Although no adverse effects were observed in any of these studies, the drug failed the phase II trial due to a lack of effect compared to placebo. The TGF- $\beta$ 3 dose in these trials are, however, not directly comparable to that used in the current study, due to the difference in administration methods.

BM-spared animals developed initial symptoms that were similar to those exhibited by TBI animals. However, BM-spared animals were less severely afflicted and the mortality in these groups was 6.7%, compared with 100% in the TBI groups. The association between prevention of H-ARS and recovery of GI-ARS observed in the current study agrees with previous reports of mitigation of GI-ARS after BM transplant [47–52] or limb shielding [53].

Saha et al. reported that when transplanted BM was enriched for mesenchymal stem cells, endothelial progenitor cells, and macrophages, the effect on GI-ARS rescue increased, compared to transplantation of whole BM [49]. Interestingly, they also found that the enriched BM could rescue animals subjected to a lethal dose of abdominal irradiation, even when the host BM was not irradiated. These protective effects were reduced when the BM was enriched for either macrophages or BM stromal cells alone, indicating that both cell populations were active contributors to GI rescue. Ch'ang et al. found that BM transplant after TBI triggered migration of host CD11b(+) myelomonocytic cells to the intestinal mucosa, leading to increased proliferation of stroma cells and regeneration of the GI epithelium [50]. Garg et al. observed improved recovery of host intestinal granulocytes, macrophages, and lymphocytes after BM transplant in 8.0 Gy TBI C57BL/6 mice [51]. Furthermore, they found that BM transplant inhibited radiation-induced permeabilization of the intestinal mucosa and increased the expression of tight-junction proteins. Conversely, Leibowitz et al. compared the transplant of wild type and radioresistant BM after TBI of C57BL/6 mice and concluded that BM-derived cells play a very limited role in GI-ARS rescue [54].

In an early study, Terry et al. found that rescue from GI-ARS by BM transplant was dependent on the number of BM cells injected in the animals [48]. For reference, both lower limbs together were estimated to contain around 12% of the total BM in CBAx C57BL hybrid mice [55]. The current results show that shielding a relatively small portion of BM from radiation was enough to increase survival from 0% to 93.3% after 8.5 Gy TBI and that BM shielding is a practically feasible and non-invasive alternative to BM transplant in preclinical studies.

When small intestine sections from TBI animals were examined histologically, the observed damage did not indicate severe depletion of intestinal crypts. However, the optimal time point to assess crypt damage in GI-ARS is days 3–4 after irradiation, compared to necropsies performed on days 7–9 in the current study [28,56]. The study would, therefore, have benefited from a sampling point to assess GI damage on day 3 after irradiation. Currently, the possibility of severe crypt damage cannot be excluded, as the turnover time for GI epithelial cells is between three and five days, and GI damage is restored within a few days after its peak [9,57]. In addition, villus density was lowered compared to non-irradiated controls, suggesting recent crypt damage. In BM-spared animals sacrificed on day 73 or 110 after irradiation, any acute GI damage can be assumed to be restored, and no direct comparison can be made between these and TBI animals that died on days 7–9. However, villus density appeared to be somewhat lowered in BM-spared animals compared to non-irradiated controls, suggesting that crypt damage may have been present at an earlier time in these animals as well.

#### 4.2. Fibrogenesis In Vitro and In Bone Marrow-Spared Animals

RIF is a potentially debilitating late toxicity in survivors of ARS, which may also considerably affect the quality of life for cancer patients after receiving radiotherapy [10]. TGF- $\beta$ 1 is one of the key mediators of RIF [10,58]. In contrast to TGF- $\beta$ 1, TGF- $\beta$ 3 is generally considered an antifibrotic cytokine [59–65], but several studies have reported pro-fibrotic effects of TGF- $\beta$ 3 [66–68]. Recombinant TGF- $\beta$ 3 was developed as a clinical anticarring agent under the name Avotermin but failed phase III trials [69]. However, no adverse effects of the drug was observed in these trials [70–72]. This ambiguity calls for a consideration of the effects of TGF- $\beta$ 3 on late radiotoxicity when evaluating its acute radioprotective or mitigating effects. We therefore investigated the effects of TGF- $\beta$ 3 and radiation on  $\alpha$ -SMA expression in vitro in addition to analyzing the collagen content in the lungs and liver of animals surviving BM-spared irradiation.

Pre-treatment of cultured MRC-5 cells with TGF- $\beta$ 3 increased the expression of the early fibrosis marker  $\alpha$ -SMA in a synergistic and dose-dependent manner when given before a single 3.5 Gy irradiation. Incubation with TGF- $\beta$ 3 without subsequent irradiation did not affect  $\alpha$ -SMA expression. These results indicate that TGF- $\beta$ 3 increased the pro-fibrotic effect of 3.5 Gy irradiation in MRC-5 cells. To the best of our knowledge, the effect of the interaction between TGF- $\beta$ 3 and ionizing radiation on  $\alpha$ -SMA expression has not been reported. The effect of TGF- $\beta$ 3 on in vitro  $\alpha$ -SMA expression, however, appears to vary depending on the model system. TGF- $\beta$ 3 treatment increased the expression of  $\alpha$ -SMA mRNA or protein in cultured human trabecular meshwork cells, urinary tract stroma-derived fibroblasts, human uterine fibroid smooth muscle cells, and 3D cultured human corneal fibroblasts (although to a lesser degree than TGF- $\beta$ 1) [73–76]. In contrast, TGF- $\beta$ 3 treatment in concentrations of 1–100 ng/mL did not increase  $\alpha$ -SMA protein content in bovine keratocyte or wounded corneal organ cultures, although TGF- $\beta$ 1 did [77]. In primary human hypertrophic fibroblasts, TGF- $\beta$ 3 treatment decreased  $\alpha$ -SMA expression [78].

The C57BL/6 mouse strain is susceptible to the development of RIF [11], and female mice appear to be more radiosensitive than males [79]. Radiation-induced hepatic fibrosis has been observed as early as one week after single-dose irradiations [79,80] and pulmonary fibrosis after one month [30] in C57BL/6 mice. In the current study, no increase in lung or liver collagen content could be observed in surviving BM-spared mice 73 or 110 days after irradiation, compared to non-irradiated age-matched mice from another experiment. In the lungs, this may be due to the relatively low dose delivered in the current experiment, as thoracic irradiation of 20 Gy is generally considered sufficient to induce pulmonary fibrosis in C57BL/6 models [11]. In the liver, however, a single total body or upper abdominal irradiation of 6 Gy has been shown to induce hepatic fibrosis in C57BL/6 mice [79,81].

In the current study, no effect from a single  $\sim$ 12.5  $\mu$ g/kg TGF- $\beta$ 3 i.v. injection could be observed on the amount of collagen in the lung or liver from BM-spared animals. Previously, weekly i.p. injections of TGF- $\beta$ 3 at a dose of 1  $\mu$ g/kg was shown to decrease the severity

and delay the onset of radiation-induced pulmonary fibrosis in mice [30]. In contrast, in a recently published study, we found indications of increased salivary gland fibrosis after daily i.p. injections of TGF- $\beta$ 3 at ~12.5  $\mu$ g/kg in a C57BL/6J mouse model of fractionated head and neck radiotherapy [37]. The differences in outcome regarding fibrogenesis in these studies may have been influenced by the differences in TGF- $\beta$ 3 doses, administration methods, or treatment regimes. While several reports exist of TGF- $\beta$ 3 reducing cutaneous scar formation in mice, rats, and humans, these studies have generally employed local injections, and thus the dose is not directly comparable [60,70,71,82–85].

Finally, increased levels of TGF- $\beta$ 3 have been observed in C57BL/6 mouse lung and Sprague-Dawley rat liver after irradiation preceding RIF but it is not clear whether TGF- $\beta$ 3 contributes to the pathological development of fibrosis or if it is part of a biological response to tissue injury [86–89].

#### 4.3. Evaluation of Animal Monitoring Methods

Due to the particularly severe impact of ARS on animal welfare, the use of humane endpoints to minimize suffering is crucial. In the current study, pain scoring according to a system developed by Nunamaker et al. [34] was used initially, and severe and progressing loss of body weight was included on day 5 after reconsideration based on animal monitoring. During the experiment, two animals died without intervention, overnight, and without meeting humane endpoints at the previous welfare check. While these two animals would have benefited from lower thresholds of humane endpoints, this would also entail euthanasia of animals that would otherwise have recovered later, affecting the results of the study. However, in retrospect, it is clear that body weight monitoring was necessary in addition to pain scoring for this animal model.

In addition to pain score and body weight, a 30% decline in body temperature relative to day 0 was used as an independent humane endpoint. This decision was based on reports that a 20–40% drop in body temperature, measured by implanted microchips, could be observed between two and four days before male CD2F1 mice reached body weight-based humane endpoints [90]. In the current study, no clear patterns of changes in body temperature were observed for any of the treatment groups. This discrepancy could be explained by differences in animal models, body temperature detection methods, or both. However, microchip implantation is an invasive procedure that itself impacts animal welfare, and the necessity of this procedure should be carefully considered in future studies, given that less invasive animal welfare assessment methods exist. Weak negative correlations were found between change in body temperature and pain score, and change in body temperature and change in body weight for both TBI and BM-spared animals. However, these correlations were too weak to be of any predictive value, and change in body temperature did not correlate with survival.

The presence of myoclonus from day 67 after irradiation in surviving BM-spared mice correlated positively with pain scores in the same mice. This may be an indication that myoclonus in itself entailed increased pain for the animals, but the possibility of observer bias cannot be excluded, as the same technician recorded clinical symptoms and pain expression in one welfare assessment. The presence of myoclonus also correlated weakly with weight gain in the same animals. However, as myoclonus was observed more frequently as the study progressed, and age-dependent weight gain is well known in C57BL/6 mice [91], there is a strong possibility that correlation was spurious with time as the confounding factor.

#### 4.4. Study Limitations

The current study has several limitations that should be considered when assessing its impact. First, the sample size is small with five mice per treatment group, making the results vulnerable to inter-animal variations. The sample size was calculated based on the pilot study described in Supplementary S1. However, the pilot study was performed with mice from a different strain that were bred and stalled in a non-barrier unit, resulting in

a different gut microbiome status compared to the animals in the present study. Second, the current study used only one irradiation dose. As mentioned, this dose may have been too high to facilitate protection against GI radiation damage by TGF- $\beta$ 3, and the study would have benefited from several doses to establish a dose–response relationship. An investigation of several dose rates or radiation qualities would also have been relevant to assess the effects of TGF- $\beta$ 3 treatment on the development of ARS. Finally, only female mice were used in this study. Sex is a potential confounder in studies of radiation sensitivity, and the possibility of different results of the current study had male mice been used cannot be excluded [92].

## 5. Conclusions

The aim of the current study was to examine whether TGF- $\beta$ 3 treatment could provide protection from or mitigation of ARS in C57BL/6J mice subjected to an 8.5 Gy TBI dose with or without shielding of the femur and BM sparing. However, all TBI animals died from GI-ARS within 10 days after irradiation, regardless of TGF- $\beta$ 3 treatment. The lack of GI radioprotection associated with TGF- $\beta$ 3 treatment in the current study may have been influenced by the gut microbiome status of the animals. BM-spared animals displayed milder progress of GI-ARS than TBI animals, in accordance with previous reports. Surprisingly, no indications of fibrosis in the form of increased collagen deposition could be observed in the lungs or livers of BM-spared animals sacrificed on day 73 or 110 after irradiation. TGF- $\beta$ 3 treatment did not affect clinical symptoms, progress of GI-ARS, or fibrogenesis in BM-spared animals. In vitro, TGF- $\beta$ 3 treatment increased  $\alpha$ -SMA expression in lung fibroblast MRC5 cells in a dose-dependent and synergistic manner when applied together with 3.5 Gy irradiation, and did not affect  $\alpha$ -SMA expression when applied alone.

**Supplementary Materials:** The following supporting information can be downloaded at: <https://www.mdpi.com/article/10.3390/applbiosci3020011/s1>, File S1: Pilot Study; File S2:  $\alpha$ -SMA detection protocol.

**Author Contributions:** Conceptualization, N.F.J.E.; methodology, I.H., N.F.J.E. and J.T.V.; formal analysis, I.H.; investigation, I.H. and J.T.V.; resources, N.F.J.E.; data curation, I.H.; writing—original draft preparation, I.H.; writing—review and editing, N.F.J.E.; visualization, I.H.; supervision, N.F.J.E.; project administration, N.F.J.E. All authors have read and agreed to the published version of the manuscript.

**Funding:** This research received no external funding.

**Institutional Review Board Statement:** The animal study protocol was approved by the Norwegian Food Safety Authority according to the EU directive 2010/63 (Protocol code/FOTS ID: 25032, approved 4 January 2021).

**Data Availability Statement:** The data from this study have been deposited to Zenodo and assigned the identifier <https://doi.org/10.5281/zenodo.10478647> (accessed on 10 January 2024).

**Acknowledgments:** We thank Olga Zlygosteva, Delmon Arous, and Kathinka E. Pitman for their help with dosimetry, irradiations, and animal welfare monitoring. We thank Mette S. Førsund at the Department of Pathology, Oslo University Hospital for help with tissue processing, sectioning, and H&E staining. We thank Inga S. Juvkam at the Institute of Oral Biology, University of Oslo for help with Masson’s Trichrome tissue staining. We thank Tine M. Søland at the Institute of Oral Biology, University of Oslo for help with the interpretation of intestine histology. We thank Čestmír Altaner and Peter Ebbesen for performing the animal experiments described in the Supporting information File S1: Pilot study.

**Conflicts of Interest:** The authors declare no conflicts of interest.

## References

1. i Garau, M.M.; Lucas Calduch, A.; López, E.C. Radiobiology of the acute radiation syndrome. *Rep. Pract. Oncol. Radiother.* **2011**, *16*, 123–130. [\[CrossRef\]](#)
2. Hall, E.J.; Giaccia, A.J. Acute Radiation Syndrome. In *Radiobiology for the Radiologist*, 7th ed.; Wolters Kluwer Health/Lipincott Williams & Wilkins: Philadelphia, PA, USA, 2012; pp. 114–128.
3. International Atomic Energy Agency. *Diagnosis and Treatment of Radiation Injuries*; Safety Reports Series No. 2; International Atomic Energy Agency: Vienna, Austria, 1998.
4. Farese, A.M.; MacVittie, T.J. Filgrastim for the treatment of hematopoietic acute radiation syndrome. *Drugs Today* **2015**, *51*, 537–548. [\[CrossRef\]](#) [\[PubMed\]](#)
5. Legesse, B.; Kaur, A.; Kenchegowda, D.; Hritzo, B.; Culp, W.E.; Moroni, M. Neulasta Regimen for the Hematopoietic Acute Radiation Syndrome: Effects Beyond Neutrophil Recovery. *Int. J. Radiat. Oncol. Biol. Phys.* **2019**, *103*, 935–944. [\[CrossRef\]](#) [\[PubMed\]](#)
6. Lazarus, H.M.; McManus, J.; Gale, R.P. Sargramostim in acute radiation syndrome. *Expert Opin. Biol. Ther.* **2022**, *22*, 1345–1352. [\[CrossRef\]](#) [\[PubMed\]](#)
7. Singh, V.K.; Seed, T.M. An update on romiplostim for treatment of acute radiation syndrome. *Drugs Today* **2022**, *58*, 133–145. [\[CrossRef\]](#) [\[PubMed\]](#)
8. US Food and Drug Administration. *Radiological and Nuclear Emergency Preparedness Information from FDA: Medical Countermeasures*; US Food and Drug Administration: Silver Spring, MD, USA, 2023.
9. Booth, C.; Tudor, G.; Tudor, J.; Katz, B.P.; MacVittie, T.J. The acute gastrointestinal syndrome in high-dose irradiated mice. *Health Phys.* **2012**, *103*, 383–399. [\[CrossRef\]](#) [\[PubMed\]](#)
10. Straub, J.M.; New, J.; Hamilton, C.D.; Lominska, C.; Shnyder, Y.; Thomas, S.M. Radiation-induced fibrosis: Mechanisms and implications for therapy. *J. Cancer Res. Clin. Oncol.* **2015**, *141*, 1985–1994. [\[CrossRef\]](#)
11. Jin, H.; Yoo, Y.; Kim, Y.; Kim, Y.; Cho, J.; Lee, Y.S. Radiation-induced lung fibrosis: Preclinical animal models and therapeutic strategies. *Cancers* **2020**, *12*, 1561. [\[CrossRef\]](#) [\[PubMed\]](#)
12. Derynck, R.; Lindquist, P.B.; Lee, A.; Wen, D.; Tamm, J.; Graycar, J.L.; Rhee, L.; Mason, A.J.; Miller, D.A.; Coffey, R.J. A new type of transforming growth factor-beta, TGF-beta 3. *EMBO J.* **1988**, *7*, 3737–3743. [\[CrossRef\]](#)
13. Ten Dijke, P.; Hansen, P.; Iwata, K.K.; Pieler, C.; Foulkes, J.G. Identification of another member of the transforming growth factor type beta gene family. *Proc. Natl. Acad. Sci. USA* **1988**, *85*, 4715–4719. [\[CrossRef\]](#)
14. Shi, Y.; Massagué, J. Mechanisms of TGF- $\beta$  Signaling from Cell Membrane to the Nucleus. *Cell* **2003**, *113*, 685–700. [\[CrossRef\]](#) [\[PubMed\]](#)
15. Wrighton, K.H.; Lin, X.; Feng, X.-H. Phospho-control of TGF-beta superfamily signaling. *Cell Res.* **2009**, *19*, 8–20. [\[CrossRef\]](#) [\[PubMed\]](#)
16. Yang, L.T.; Kaartinen, V. Tgfb1 expressed in the Tgfb3 locus partially rescues the cleft palate phenotype of Tgfb3 null mutants. *Dev. Biol.* **2007**, *312*, 384–395. [\[CrossRef\]](#) [\[PubMed\]](#)
17. Komai, T.; Okamura, T.; Inoue, M.; Yamamoto, K.; Fujio, K. Reevaluation of pluripotent cytokine TGF- $\beta$ 3 in immunity. *Int. J. Mol. Sci.* **2018**, *19*, 2261. [\[CrossRef\]](#) [\[PubMed\]](#)
18. Hanson, I.; Pitman, K.E.; Edin, N.F.J. The Role of TGF- $\beta$ 3 in Radiation Response. *Int. J. Mol. Sci.* **2023**, *24*, 7614. [\[CrossRef\]](#) [\[PubMed\]](#)
19. Kaartinen, V.; Voncken, J.W.; Shuler, C.; Warburton, D.; Bu, D.; Heisterkamp, N.; Groffen, J. Abnormal lung development and cleft palate in mice lacking TGF- $\beta$ 3 indicates defects of epithelial-mesenchymal interaction. *Nat. Genet.* **1995**, *11*, 415–421. [\[CrossRef\]](#) [\[PubMed\]](#)
20. Proetzel, G.; Pawlowski, S.A.; Wiles, M.V.; Yin, M.; Boivin, G.P.; Howles, P.N.; Ding, J.; Ferguson, M.W.J.; Doetschman, T. Transforming growth factor- $\beta$ 3 is required for secondary palate fusion. *Nat. Genet.* **1995**, *11*, 409–414. [\[CrossRef\]](#)
21. Laverty, H.G.; Wakefield, L.M.; Ocleston, N.L.; O’Kane, S.; Ferguson, M.W.J. TGF- $\beta$ 3 and cancer: A review. *Cytokine Growth Factor Rev.* **2009**, *20*, 305–317. [\[CrossRef\]](#) [\[PubMed\]](#)
22. Robson, H.; Spence, K.; Anderson, E.; Potten, C.S.; Hendry, J.H. Differential influence of TGF $\beta$ 1 and TGF $\beta$ 3 isoforms on cell cycle kinetics and postirradiation recovery of normal and malignant colorectal epithelial cells. *Int. J. Radiat. Oncol.* **1997**, *38*, 183–190. [\[CrossRef\]](#)
23. Khalil, N.; O’Connor, R.N.; Flanders, K.C.; Shing, W.; Whitman, C.I. Regulation of type II alveolar epithelial cell proliferation by TGF- $\beta$  during bleomycin-induced lung injury in rats. *Am. J. Physiol.-Lung Cell. Mol. Physiol.* **1994**, *267*, 498–507. [\[CrossRef\]](#)
24. McCormack, E.S.; Borzillo, G.V.; Ambrosino, C.; Mak, G.; Hamablet, L.; Qu, G.Y.; Haley, J.D. Transforming growth factor- $\beta$ 3 protection of epithelial cells from cycle-selective chemotherapy in vitro. *Biochem. Pharmacol.* **1997**, *53*, 1149–1159. [\[CrossRef\]](#) [\[PubMed\]](#)
25. Nakamura, S.I.; Kawai, T.; Kamakura, T.; Ookura, T. TGF- $\beta$ 3 is expressed in taste buds and inhibits proliferation of primary cultured taste epithelial cells. *In Vitro Cell. Dev. Biol.-Anim.* **2010**, *46*, 36–44. [\[CrossRef\]](#) [\[PubMed\]](#)
26. Edin, N.J.; Sandvik, J.A.; Cheng, C.; Bergersen, L.; Pettersen, E.O. The roles of TGF- $\beta$ 3 and peroxynitrite in removal of hyper-radiosensitivity by priming irradiation. *Int. J. Radiat. Biol.* **2014**, *90*, 527–537. [\[CrossRef\]](#) [\[PubMed\]](#)
27. Jeppesen Edin, N.; Altaner, Č.; Altanero, V.; Ebbesen, P. TGF- $\beta$ 3 Dependent Modification of Radiosensitivity in Reporter Cells Exposed to Serum from Whole-Body Low Dose-Rate Irradiated Mice. *Dose-Response* **2015**, *13*, 1–15. [\[CrossRef\]](#) [\[PubMed\]](#)

28. Potten, C.S.; Booth, D.; Haley, J.D. Pretreatment with transforming growth factor beta-3 protects small intestinal stem cells against radiation damage in vivo. *Br. J. Cancer* **1997**, *75*, 1454–1459. [[CrossRef](#)] [[PubMed](#)]
29. Booth, D.; Haley, J.D.; Bruskin, A.M.; Potten, C.S. Transforming growth factor-B3 protects murine small intestinal stem cells and animal survival after irradiation, possibly by reducing stem-cell cycling. *Int. J. Cancer* **2000**, *86*, 53–59. [[CrossRef](#)]
30. Xu, L.; Xiong, S.; Guo, R.; Yang, Z.; Wang, Q.; Xiao, F.; Wang, H.; Pan, X.; Zhu, M. Transforming growth factor  $\beta$ 3 attenuates the development of radiation-induced pulmonary fibrosis in mice by decreasing fibrocyte recruitment and regulating IFN- $\gamma$ /IL-4 balance. *Immunol. Lett.* **2014**, *162*, 27–33. [[CrossRef](#)] [[PubMed](#)]
31. Jacobs, J.P.; Jones, C.M.; Baille, J.P. Characteristics of a human diploid cell designated MRC-5. *Nature* **1970**, *227*, 168–170. [[CrossRef](#)]
32. Nunamaker, E.A.; Anderson, R.J.; Artwohl, J.E.; Lyubimov, A.V.; Fortman, J.D. Predictive Observation-Based Endpoint Criteria for Mice Receiving Total Body Irradiation. *Comp. Med.* **2013**, *63*, 313–322.
33. Singh, V.K.; Newman, V.L.; Berg, A.N.; MacVittie, T.J. Animal models for acute radiation syndrome drug discovery. *Expert Opin. Drug Discov.* **2015**, *10*, 497–517. [[CrossRef](#)]
34. Nunamaker, E.A.; Artwohl, J.E.; Anderson, R.J.; Fortman, J.D. Endpoint Refinement for Total Body Irradiation of C57BL/6 Mice. *Comp. Med.* **2013**, *63*, 22–28. [[PubMed](#)]
35. Bankhead, P.; Loughrey, M.B.; Fernández, J.A.; Dombrowski, Y.; McArt, D.G.; Dunne, P.D.; McQuaid, S.; Gray, R.T.; Murray, L.J.; Coleman, H.G.; et al. QuPath: Open source software for digital pathology image analysis. *Sci. Rep.* **2017**, *7*, 16878. [[CrossRef](#)] [[PubMed](#)]
36. Schneider, C.A.; Rasband, W.S.; Eliceiri, K.W. NIH Image to ImageJ: 25 years of image analysis. *Nat. Methods* **2012**, *9*, 671–675. [[CrossRef](#)] [[PubMed](#)]
37. Hanson, I.; Juvkam, I.S.; Zlygosteva, O.; Søland, T.M.; Galtung, H.K.; Malinen, E.; Edin, N.F.J. TGF- $\beta$ 3 increases the severity of radiation-induced oral mucositis and salivary gland fibrosis in a mouse model. *Int. J. Radiat. Biol.* **2024**; *Online ahead of print.* [[CrossRef](#)]
38. Kendall tau Rank Correlation (v1.0.13). 2017. Available online: <https://www.wessa.net/> (accessed on 4 March 2024).
39. Juvkam, I.S.; Zlygosteva, O.; Malinen, E.; Edin, N.J.; Galtung, H.K.; Søland, T.M. Fractionated irradiation of murine salivary glands resulted in focal acinar cell atrophy, immune cell infiltration, fibrosis, and hyposalivation. *BioRxiv* **2023**. [[CrossRef](#)]
40. Juvkam, I.S.; Zlygosteva, O.; Arous, D.; Galtung, H.K.; Malinen, E.; Søland, T.M.; Jeppesen Edin, N. A preclinical model to investigate normal tissue damage following fractionated radiotherapy to the head and neck. *J. Radiat. Res.* **2022**, *64*, 44–52. [[CrossRef](#)] [[PubMed](#)]
41. Plett, P.A.; Sampson, C.H.; Lin Chua, H.; Joshi, M.; Booth, C.; Gough, A.; Johnson, C.S.; Katz, B.P.; Farese, A.M.; Parker, J.; et al. Establishing a murine model of the Hematopoietic Syndrome of the Acute Radiation Syndrome. *Health Phys.* **2012**, *103*, 343–355. [[CrossRef](#)] [[PubMed](#)]
42. Jian, Y.; Zhang, D.; Liu, M.; Wang, Y.; Xu, Z.X. The Impact of Gut Microbiota on Radiation-Induced Enteritis. *Front. Cell. Infect. Microbiol.* **2021**, *11*, 586392. [[CrossRef](#)] [[PubMed](#)]
43. Liu, J.; Liu, C.; Yue, J. Radiotherapy and the gut microbiome: Facts and fiction. *Radiat. Oncol.* **2021**, *16*, 9. [[CrossRef](#)] [[PubMed](#)]
44. Yu, Y.; Lin, X.; Feng, F.; Wei, Y.; Wei, S.; Gong, Y.; Guo, C.; Wang, Q.; Shuai, P.; Wang, T.; et al. Gut microbiota and ionizing radiation-induced damage: Is there a link? *Environ. Res.* **2023**, *229*, 115947. [[CrossRef](#)]
45. Wymenga, A.N.M.; van der Graaf, W.T.A.; Hofstra, L.S.; Spijkervet, F.K.L.; Timens, W.; Timmer-Bosscha, H.; Sluiter, W.J.; van Buuren, A.H.J.A.W.; Mulder, N.H.; de Vries, E.G.E. Phase I Study of Transforming Growth Factor-3 Mouthwashes for Prevention of Chemotherapy-induced Mucositis. *Clin. Cancer Res.* **1999**, *5*, 1363–1368.
46. Foncuberta, M.C.; Cagnoni, P.J.; Brandts, C.H.; Mandanas, R.; Fields, K.; Derigs, H.G.; Reed, E.; Sonis, S.T.; Fay, J.; LeVeque, F.; et al. Topical Transforming Growth Factor- $\beta$ 3 in the Prevention or Alleviation of Chemotherapy-Induced Oral Mucositis in Patients with Lymphomas or Solid Tumors. *J. Immunother.* **2001**, *24*, 384–388. [[CrossRef](#)] [[PubMed](#)]
47. Mason, K.A.; Withers, H.R.; McBride, W.H.; Davis, C.A.; Smathers, J.B. Comparison of the gastrointestinal syndrome after total-body or total-abdominal irradiation. *Radiat. Res.* **1989**, *117*, 480–488. [[CrossRef](#)] [[PubMed](#)]
48. Terry, N.H.A.; Travis, E.L. The influence of bone marrow depletion on intestinal radiation damage. *Int. J. Radiat. Oncol. Biol. Phys.* **1989**, *17*, 569–573. [[CrossRef](#)] [[PubMed](#)]
49. Saha, S.; Bhanja, P.; Kabarriti, R.; Liu, L.; Alfieri, A.A.; Guha, C. Bone marrow stromal cell transplantation mitigates radiation-induced gastrointestinal syndrome in mice. *PLoS ONE* **2011**, *6*, e24072. [[CrossRef](#)] [[PubMed](#)]
50. Ch'Ang, H.J.; Lin, L.M.; Chang, P.Y.; Luo, C.W.; Chang, Y.H.; Chou, C.K.; Chen, H.H. Bone marrow transplantation enhances trafficking of host-derived myelomonocytic cells that rescue intestinal mucosa after whole body radiation. *Radiother. Oncol.* **2012**, *104*, 401–407. [[CrossRef](#)] [[PubMed](#)]
51. Garg, S.; Wang, W.; Prabath, B.G.; Boerma, M.; Wang, J.; Zhou, D.; Hauer-Jensen, M. Bone marrow transplantation helps restore the intestinal mucosal barrier after total body irradiation in mice. *Radiat. Res.* **2014**, *181*, 229–239. [[CrossRef](#)] [[PubMed](#)]
52. Pejchal, J.; Šinkorová, Z.; Tichý, A.; Kmočová, A.; Ďurišová, K.; Kubelková, K.; Pohanka, M.; Bureš, J.; Tachecí, I.; Kuča, K.; et al. Attenuation of radiation-induced gastrointestinal damage by epidermal growth factor and bone marrow transplantation in mice. *Int. J. Radiat. Biol.* **2015**, *91*, 703–714. [[CrossRef](#)]
53. Brodin, N.P.; Velcich, A.; Guha, C.; Tomé, W.A.; Tomé, T. A Model for Precise and Uniform Pelvic-and Limb-Sparing Abdominal Irradiation to Study the Radiation-Induced Gastrointestinal Syndrome in Mice Using Small Animal Irradiation Systems. *Dose-Response* **2017**, *15*, 1559325816685798. [[CrossRef](#)] [[PubMed](#)]

54. Leibowitz, B.J.; Wei, L.; Zhang, L.; Ping, X.; Epperly, M.; Greenberger, J.; Cheng, T.; Yu, J. Ionizing irradiation induces acute haematopoietic syndrome and gastrointestinal syndrome independently in mice. *Nat. Commun.* **2014**, *5*, 3494. [CrossRef]
55. Shaposhnikov, V.L. Distribution of bone marrow cells in the mouse skeleton. *Bull. Exp. Biol. Med.* **1979**, *87*, 510–512. [CrossRef]
56. Withers, H.R.; Elkind, M.M. Microcolony Survival Assay for Cells of Mouse Intestinal Mucosa Exposed to Radiation. *Int. J. Radiat. Biol. Relat. Stud. Phys. Chem. Med.* **1970**, *17*, 261–267. [CrossRef] [PubMed]
57. Potten, C.S. Radiation, the Ideal Cytotoxic Agent for Studying the Cell Biology of Tissues such as the Small Intestine. *Radiat. Res.* **2004**, *161*, 123–136. [CrossRef] [PubMed]
58. Martin, M.; Lefaix, J.-L.; Sylvie, D. TGF-beta1 and radiation fibrosis: A master switch and a specific therapeutic target? *Int. J. Radiat. Oncol.* **2000**, *47*, 277–290. [CrossRef] [PubMed]
59. Serini, G.; Gabbiani, G. Modulation of  $\alpha$ -smooth muscle actin expression in fibroblasts by transforming growth factor-P isoforms: An in vivo and in vitro study. *Wound Repair. Regen.* **1996**, *3*, 278–287. [CrossRef] [PubMed]
60. Loewen, M.S.; Walner, D.L.; Caldarelli, D.D. Improved airway healing using transforming growth factor beta-3 in a rabbit model. *Wound Repair. Regen.* **2001**, *9*, 44–49. [CrossRef] [PubMed]
61. Ask, K.; Bonniaud, P.; Maass, K.; Eickelberg, O.; Margetts, P.J.; Warburton, D.; Groffen, J.; Gauldie, J.; Kolb, M. Progressive pulmonary fibrosis is mediated by TGF- $\beta$  isoform 1 but not TGF- $\beta$ 3. *Int. J. Biochem. Cell Biol.* **2008**, *40*, 484–495. [CrossRef] [PubMed]
62. Wu, Y.; Peng, Y.; Gao, D.; Feng, C.; Yuan, X.; Li, H.; Wang, Y.; Yang, L.; Huang, S.; Fu, X. Mesenchymal Stem Cells Suppress Fibroblast Proliferation and Reduce Skin Fibrosis through a TGF- $\beta$ 3-Dependent Activation. *Int. J. Low. Extrem. Wounds* **2015**, *14*, 50–62. [CrossRef]
63. Xue, K.; Zhang, J.; Li, C.; Li, J.; Wang, C.; Zhang, Q.; Chen, X.; Yu, X.; Sun, L.; Yu, X. The role and mechanism of transforming growth factor beta 3 in human myocardial infarction-induced myocardial fibrosis. *J. Cell. Mol. Med.* **2019**, *23*, 4229–4243. [CrossRef] [PubMed]
64. Escasany, E.; Lanzón, B.; García-Carrasco, A.; Izquierdo-Lahuerta, A.; Torres, L.; Corrales, P.; Rodríguez, A.E.R.; Luis-Lima, S.; Álvarez, C.M.; Ruperez, F.J.; et al. Transforming growth factor  $\beta$  3 deficiency promotes defective lipid metabolism and fibrosis in murine kidney. *Dis. Model. Mech.* **2021**, *14*, dmm048249. [CrossRef]
65. Wilson, S.E. TGF beta -1, -2 and -3 in the modulation of fibrosis in the cornea and other organs. *Exp. Eye Res.* **2021**, *207*, 108594. [CrossRef]
66. Reggio, S.; Rouault, C.; Poitou, C.; Bichet, J.-C.; Prifti, E.; Bouillot, J.-L.; Rizkalla, S.; Lacasa, D.; Tordjman, J.; Clément, K. Increased Basement Membrane Components in Adipose Tissue During Obesity: Links With TGF and Metabolic Phenotypes. *J. Clin. Endocrinol. Metab.* **2016**, *101*, 2578–2587. [CrossRef] [PubMed]
67. Guo, J.; Liu, W.; Zeng, Z.; Lin, J.; Zhang, X.; Chen, L. Tgfb3 and Mmp13 regulated the initiation of liver fibrosis progression as dynamic network biomarkers. *J. Cell. Mol. Med.* **2021**, *25*, 867–879. [CrossRef] [PubMed]
68. Sun, T.; Huang, Z.; Liang, W.C.; Yin, J.; Lin, W.Y.; Wu, J.; Vernes, J.M.; Lutman, J.; Caplazi, P.; Jeet, S.; et al. TGF $\beta$ 2 and TGF $\beta$ 3 isoforms drive fibrotic disease pathogenesis. *Sci. Transl. Med.* **2021**, *13*, eabe0407. [CrossRef] [PubMed]
69. Juvista EU Phase 3 Trial Results. *Fierce Biotech*. 2011. Available online: <https://www.fiercebiotech.com/biotech/juvista-eu-phase-3-trial-results> (accessed on 13 March 2023).
70. Ferguson, M.W.; Duncan, J.; Bond, J.; Bush, J.; Durani, P.; So, K.; Taylor, L.; Chantrey, J.; Mason, T.; James, G.; et al. Prophylactic administration of avotermin for improvement of skin scarring: Three double-blind, placebo-controlled, phase I/II studies. *Lancet* **2009**, *373*, 1264–1274. [CrossRef] [PubMed]
71. Bush, J.; Duncan, J.A.L.; Bond, J.S.; Durani, P.; So, K.; Mason, T.; O’Kane, S.; Ferguson, M.W.J. Scar-Improving Efficacy of Avotermin Administered into the Wound margins of Skin Incisions as Evaluated by a Randomized, Double-Blind, Placebo-Controlled, Phase II Clinical Trial. *Plast. Reconstr. Surg.* **2010**, *126*, 1604–1615. [CrossRef] [PubMed]
72. So, K.; McGrouther, D.A.; Bush, J.A.; Durani, P.; Taylor, L.; Skotny, G.; Mason, T.; Metcalfe, A.; Okane, S.; Ferguson, M.W.J. Avotermin for scar improvement following scar revision surgery: A randomized, double-blind, within-patient, placebo-controlled, phase II clinical trial. *Plast. Reconstr. Surg.* **2011**, *128*, 163–172. [CrossRef] [PubMed]
73. Heer, R.; Clarke, N.; Rigas, A.C.; Cheek, T.R.; Pickard, R.; Leung, H.Y. Phenotypic modulation of human urinary tract stroma-derived fibroblasts by transforming growth factor  $\beta$ 3. *Urology* **2010**, *76*, 509.e13–509.e20. [CrossRef] [PubMed]
74. Salama, S.A.; Diaz-Arrastia, C.R.; Kilic, G.S.; Kamel, M.W. 2-Methoxyestradiol causes functional repression of transforming growth factor  $\beta$ 3 signaling by ameliorating Smad and non-Smad signaling pathways in immortalized uterine fibroid cells. *Fertil. Steril.* **2012**, *98*, 178–184.e1. [CrossRef]
75. Yeung, V.; Sriram, S.; Tran, J.A.; Guo, X.; Hutcheon, A.E.K.; Zieske, J.D.; Karamichos, D.; Ciolino, J.B. Fak inhibition attenuates corneal fibroblast differentiation in vitro. *Biomolecules* **2021**, *11*, 1682. [CrossRef]
76. Liu, M.; Honjo, M.; Yamagishi, R.; Igarashi, N.; Nakamura, N.; Kurano, M.; Yatomi, Y.; Igarashi, K.; Aihara, M. Fibrotic Response of Human Trabecular Meshwork Cells to Transforming Growth Factor-Beta 3 and Autotaxin in Aqueous Humor. *Biomolecules* **2022**, *12*, 1231. [CrossRef]
77. Carrington, L.M.; Albon, J.; Anderson, I.; Kamma, C.; Boulton, M. Differential regulation of key stages in early corneal wound healing by TGF- $\beta$  isoforms and their inhibitors. *Investig. Ophthalmol. Vis. Sci.* **2006**, *47*, 1886–1894. [CrossRef] [PubMed]
78. Lee, J.S.; Cho, H.G.; Lee, J.W.; Oh, E.J.; Kim, H.M.; Ko, U.H.; Kang, M.; Shin, J.H.; Chung, H.Y. Influence of Transforming Growth Factors beta 1 and beta 3 in the Scar Formation Process. *J. Craniofac. Surg.* **2023**, *34*, 904–909. [CrossRef] [PubMed]

79. Wang, S.; Lee, K.; Hyun, J.; Lee, Y.; Kim, Y.; Jung, Y. Hedgehog signaling influences gender-specific response of liver to radiation in mice. *Hepatol. Int.* **2013**, *7*, 1065–1074. [[CrossRef](#)] [[PubMed](#)]
80. Wang, S.; Hyun, J.; Youn, B.; Jung, Y. Hedgehog signaling regulates the repair response in mouse liver damaged by irradiation. *Radiat. Res.* **2013**, *179*, 69–75. [[CrossRef](#)] [[PubMed](#)]
81. Wang, S.; Lee, Y.; Kim, J.; Hyun, J.; Lee, K. Potential Role of Hedgehog Pathway in Liver Response to Radiation. *PLoS ONE* **2013**, *8*, e74141. [[CrossRef](#)] [[PubMed](#)]
82. Shah, M.; Foreman, D.; Ferguson, M.W.J. Neutralisation of TGF- $\beta$ 1 and TGF- $\beta$ 2 or exogenous addition of TGF- $\beta$ 3 to cutaneous rat wounds reduces scarring. *J. Cell Sci.* **1995**, *108*, 985–1002. [[CrossRef](#)]
83. Lanning, D.A.; Diegelmann, R.F.; Yager, D.R.; Wallace, M.L.; Bagwell, C.E.; Haynes, J.H. Myofibroblast induction with transforming growth factor- $\beta$ 1 and - $\beta$ 3 in cutaneous fetal excisional wounds. *J. Pediatr. Surg.* **2000**, *35*, 183–188. [[CrossRef](#)]
84. Hosokawa, R.; Nonaka, K.; Morifuji, M.; Shum, L.; Ohishi, M. TGF- $\beta$ 3 Decreases Type I Collagen and Scarring after Labioplasty. *J. Dent. Res.* **2003**, *82*, 558–564. [[CrossRef](#)] [[PubMed](#)]
85. Chang, Z.; Kishimoto, Y.; Hasan, A.; Welham, N. V TGF- $\beta$ 3 modulates the inflammatory environment and reduces scar formation following vocal fold mucosal injury in rats. *Dis. Model. Mech.* **2014**, *7*, 83–91. [[CrossRef](#)]
86. Finkelstein, J.N.; Johnston, C.J.; Baggs, R.; Rubin, P. Early alterations in extracellular matrix and transforming growth factor  $\beta$  gene expression in mouse lung indicative of late radiation fibrosis. *Int. J. Radiat. Oncol.* **1994**, *28*, 621–631. [[CrossRef](#)]
87. Johnston, C.J.; Piedboeuf, B.; Baggs, R.; Rubin, P.; Finkelstein, J.N. Differences in Correlation of mRNA Gene Expression in Mice Sensitive and Resistant to Radiation-Induced Pulmonary Fibrosis. *Radiat. Res.* **1995**, *142*, 197–203. [[CrossRef](#)] [[PubMed](#)]
88. Rubin, P.; Johnston, C.J.; Williams, J.P.; McDonald, S.; Finkelstein, J.N. A perpetual cascade of cytokines postirradiation leads to pulmonary fibrosis. *Int. J. Radiat. Oncol.* **1995**, *33*, 99–109. [[CrossRef](#)] [[PubMed](#)]
89. Seong, J.; Kim, S.H.; Chung, E.J.; Lee, W.J.; Suh, C.O. Early alteration in TGF- $\beta$  mRNA expression in irradiated rat liver. *Int. J. Radiat. Oncol.* **2000**, *46*, 639–643. [[CrossRef](#)] [[PubMed](#)]
90. Koch, A.; Gulani, J.; King, G.; Hieber, K.; Chappell, M. Establishment of Early Endpoints in Mouse Total-Body Irradiation Model. *PLoS ONE* **2016**, *11*, e0161079. [[CrossRef](#)]
91. The Jackson Laboratory. Body Weight Information for C57BL/6J. 2023. Available online: <https://www.jax.org/jax-mice-and-services/strain-data-sheet-pages/body-weight-chart-000664> (accessed on 4 March 2024).
92. Taliaferro, L.P.; Agarwal, R.K.; Coleman, C.N.; Andrea, L.; Hofmeyer, K.A.; Loelius, S.G.; Molinar-inglis, O.; Tedesco, D.C.; Satyamitra, M.M.; Taliaferro, L.P.; et al. Sex differences in radiation research. *Int. J. Radiat. Biol.* **2023**, *100*, 466–485. [[CrossRef](#)]

**Disclaimer/Publisher’s Note:** The statements, opinions and data contained in all publications are solely those of the individual author(s) and contributor(s) and not of MDPI and/or the editor(s). MDPI and/or the editor(s) disclaim responsibility for any injury to people or property resulting from any ideas, methods, instructions or products referred to in the content.